J. Fluid Mech. (2001), *vol.* 443, *pp.* 351–376. Printed in the United Kingdom

© 2001 Cambridge University Press

Ageostrophic dynamics of an intense localized vortex on a β-plane

By G. M. REZNIK[1] AND R. GRIMSHAW[2]†

[1]P. P. Shirshov Institute of Oceanology, Moscow, Russia

[2]Monash University, Melbourne, Australia

(Received 18 November 1999 and in revised form 26 April 2001)

We consider the non-stationary dynamics of an intense localized vortex on a β-plane using a shallow-water model. An asymptotic theory for a vortex with piecewise-continuous potential vorticity is developed assuming the Rossby number to be small and the free surface elevation to be small but finite. Analogously to the well-known quasi-geostrophic model, the vortex translation is produced by a secondary dipole circulation (β-gyres) developed in the vortex vicinity and consisting of two parts. The first part (geostrophic β-gyres) coincides with the β-gyres in the geostrophic model, and the second (ageostrophic β-gyres) is due to ageostrophic terms in the governing equations. The time evolution of the ageostrophic β-gyres consists of fast and slow stages. During the fast stage the radiation of inertia–gravity waves results in the rapid development of the β-gyres from zero to a dipole field independent of the fast time variable. Correspondingly, the vortex accelerates practically instantaneously (compared to the typical swirling time) to some finite value of the translation speed. At the next slow stage the inertia–gravity wave radiation is insignificant and the β-gyres evolve with the typical swirling time. The total zonal translation speed induced by the geostrophic and ageostrophic β-gyres tends with increasing time to the speed of a steadily translating monopole exceeding (not exceeding) the drift velocity of Rossby waves for anticyclones (cyclones). This cyclone/anticyclone asymmetry generalizes the well-known finding about the greater longevity of anticyclones compared to cyclones to the case of non-stationary evolving monopoles. The influence of inertia–gravity waves upon the vortex evolution is analysed. The main role of these waves is to provide a 'fast' adjustment to the 'slow' vortex evolution. The energy of inertia–gravity waves is negligible compare to the energy of the geostrophic β-gyres. Yet another feature of the ageostrophic vortex evolution is that the area of the potential vorticity patch changes in the course of time, the cyclonic patch contracting and the anticyclonic one expanding.

1. Introduction

The main goal of this work is a better understanding of the influence of ageostrophic factors on the dynamics of localized mesoscale vortices in the oceans and atmospheres of the Earth and other planets. Two interrelated effects are of primary interest: (i) the presence of fast inertia–gravity waves along with slow Rossby waves, and (ii) the finite deviations of isopycnals and the free surface from their equilibrium positions. The

† Present address: Department of Mathematical Sciences, Loughborough University, Loughborough, Leicestershire LE11 3TU, UK.

https://doi.org/10.1017/S0022112001005468 Published online by Cambridge University Press

role of inertia–gravity waves in the evolution of localized mesoscale vortex is poorly understood; even a numerical investigation of this problem presents difficulties. The finite deviation of isopycnals breaks the symmetry, which characterizes the quasi-geostrophic (QG) potential vorticity equation

$$\frac{\partial}{\partial t}(\nabla^2\Psi - R_d^{-2}\Psi) + \beta\frac{\partial\Psi}{\partial x} + J(\Psi, \nabla^2\Psi) = 0 \tag{1.1}$$

(e.g. Pedlosky 1979). One can readily show that (1.1) is invariant relative to the transformation

$$x \to x, \quad y \to -y, \quad \Psi \to -\Psi. \tag{1.2}$$

Due to (1.2) the solution for a cyclone (anticyclone) can be derived from the solution for an anticyclone (cyclone) by the simple simultaneous change of the streamfunction sign and the mirror reflection with respect to the zonal axis. In other words, a cyclone and anticyclone differing only in sign are equivalent in the QG approximation. Lack of such a symmetry in an ageostrophic system results in the so-called cyclone/anticyclone asymmetry (CAA) when cyclones and anticyclones may substantially differ in their properties.

This CAA effect is of great interest since it is well known that the most persistent long-lived large-scale vortices have an anticyclonic sense of rotation. In the ocean intrathermocline lenses can exist for several years and travel distances of thousands of kilometers (McWilliams 1985; Kamenkovich, Koshlyakov & Monin 1986). Large long-lived anticyclones are observed in the atmospheres of Jupiter, Saturn and Neptune (e.g. Nezlin & Sutyrin 1994). The difference between anticyclones and cyclones has also been clearly demonstrated in laboratory (e.g. Nezlin & Sutyrin 1994) and in numerical experiments (e.g. Matsuura & Yamagata 1982; Williams & Yamagata 1984; Davey & Killworth 1984; Chassignet & Cushman-Roisin 1991).

Theoretical explanations of the CAA have focused mainly on studies of steadily translating vortices (e.g. Nof 1981; Killworth 1983, 1986; Nycander & Sutyrin 1992; Sutyrin & Dewar 1992; Stegner & Zeitlin 1996; Benilov 1996). It has been found that intense anticyclones steadily translating westward faster than linear Rossby waves can exist in shallow-water models. For cyclones the same asymptotic theory fails and the existence of analogous solutions is doubtful. The only attempt to examine the non-stationary dynamics of a localized vortex in the presence of ageostrophic factors was made by Sutyrin (1994) using a heuristic combination of intermediate geostrophic and frontal geostrophic models.

The main aim of this paper is to examine the influence of ageostrophic effects upon the non-stationary dynamics of intense monopolar vortices. To do this we generalize the model of an intense vortex with piecewise-constant potential vorticity (Sutyrin & Flierl 1994; Reznik, Grimshaw & Benilov 2000, referred to herein as RGB) from QG theory to the case of a one-layer shallow-water model and consider the evolution of such a vortex. Our main attention is focused on the time development of the CAA and the role of the fast inertia–gravity waves in the intense vortex evolution.

The paper is organized as follows. In § 2 the model is formulated. Section 3 contains a description of the initial vortex. In § 4 we discuss the asymptotic algorithm; if the reader is not interested in these mathematical details, then it is only necessary to read the introduction of § 4 (up to the first subsection), and then proceed directly to § 5. Section 5 contains the most important formulae (almost without derivation) describing the geostrophic and ageostrophic β-gyres and radiated inertia–gravity waves. Section 6 is concerned mainly with some properties of the ageostrophic

https://doi.org/10.1017/S0022112001005468 Published online by Cambridge University Press

β-gyres. The evolution of the vortex patch is considered in § 7. A summary of our results is presented in § 8. A detailed analysis of the first and second approximations is contained in Appendices A and B, while the derivation of some formulae needed to calculate the vortex patch expansion rate in § 7 is contained in Appendix C. These Appendices are available from the JFM office, or directly from either author.

2. Model

2.1. *Governing equations*

We consider the non-stationary dynamics of a localized vortex on the β-plane in the framework of a shallow-water model. The model equations, in moving coordinates attached to the vortex centre, take the form

$$\frac{\partial u}{\partial t} + (u - \dot{X})\frac{\partial u}{\partial x} + (v - \dot{Y})\frac{\partial u}{\partial y} - fv = -g'\frac{\partial h}{\partial x}, \tag{2.1a}$$

$$\frac{\partial v}{\partial t} + (u - \dot{X})\frac{\partial v}{\partial x} + (v - \dot{Y})\frac{\partial v}{\partial y} + fu = -g'\frac{\partial h}{\partial y}, \tag{2.1b}$$

$$\frac{\partial h}{\partial t} + \frac{\partial [h(u - \dot{X})]}{\partial x} + \frac{\partial [h(v - \dot{Y})]}{\partial y} = 0 \tag{2.1c}$$

Here x, y denote eastward and northward coordinates and t time; h is the layer depth; u, v are the absolute zonal and meridional velocities; g' is reduced gravity; $f = f_0 + \beta(y + Y)$ is the Coriolis parameter; $X(t), Y(t)$ are the zonal and meridional distances travelled by the vortex, $(\dot{X}, \dot{Y})$ is the vortex translation speed. The vortex path $\boldsymbol{r} = (X, Y)$ and translation speed are unknown in advance and should be determined as part of the solution.

The potential vorticity equation follows from (2.1*a–c*):

$$\frac{\partial \Pi}{\partial t} + (u - \dot{X})\frac{\partial \Pi}{\partial x} + (v - \dot{Y})\frac{\partial \Pi}{\partial y} = 0, \quad \Pi = \frac{\zeta + f}{h}, \quad \zeta = \frac{\partial v}{\partial x} - \frac{\partial u}{\partial y}, \tag{2.2}$$

where ζ and Π are the relative and potential vorticity respectively. It is convenient to introduce the new variable Ω:

$$\Omega = \frac{\zeta + f_0}{h} - \frac{f_0}{h_\infty}, \quad \text{so that} \quad \Pi = \Omega + \frac{\beta(y + Y)}{h} + \frac{f_0}{h_\infty}. \tag{2.3}$$

Here $h = \hat{h} + h_\infty$, where h_∞ denotes the limiting value of the depth h at infinity and $\hat{h}$ is the depth deviation; unlike Π the function Ω decays at infinity together with the velocity field and $\hat{h}$. The equation for Ω simply follows from (2.2):

$$\frac{\partial \Omega}{\partial t} + (u - \dot{X})\frac{\partial \Omega}{\partial x} + (v - \dot{Y})\frac{\partial \Omega}{\partial y} + \frac{\beta}{h}\left[(y + Y)\left(\frac{\partial u}{\partial x} + \frac{\partial v}{\partial y}\right) + v\right] = 0. \tag{2.4}$$

2.2. *Piecewise-continuous potential vorticity model*

We consider the case when the initial state is an axisymmetric vortex patch, i.e.

$$V = V_I(r), \quad U = 0, \quad \hat{h} = \hat{h}_I(r) \quad \text{for} \quad t = 0, \tag{2.5}$$

and the initial vortex is determined by the requirement that it satisfies equations

https://doi.org/10.1017/S0022112001005468 Published online by Cambridge University Press

(2.1*a–c*), (2.4) when $\beta = 0$, so that

$$\frac{V_I^2}{r} + f_0 V_I = g' \frac{f\hat{h}_I}{fr}, \quad \Omega_I = \frac{\zeta_I - f_0 \hat{h}_I / h_\infty}{h_\infty + \hat{h}_I} = \gamma Q H(r_I - r), \tag{2.6a, b}$$

$$\zeta_I = \frac{\mathrm{d}V_I}{\mathrm{d}r} + \frac{V_I}{r}. \tag{2.6c}$$

Here U, V are radial and azimuthal velocities in polar coordinates attached to the vortex centre, $U = u\cos\theta + v\sin\theta$, $V = -u\sin\theta + v\cos\theta$; $H(z)$ is the Heaviside function, $H(z) = 1$ if $z > 0$ and $H(z) = 0$ if $z < 0$; Q is a constant vorticity amplitude, and $\gamma = \pm 1$ for cyclones (anticyclones) respectively assuming that $f_0 > 0$ (i.e. the Northern Hemisphere convention); r_I is the initial radius, and is a constant.

At subsequent times the function Ω remains piecewise-continuous, i.e. it is represented by the form

$$\Omega = \frac{\zeta - f_0 \hat{h}/h_\infty}{h_\infty + \hat{h}} = \gamma Q H(r_b - r) + q(x, y, t), \tag{2.7}$$

where $q(x, y, t)$ is a continuous function and the patch boundary is expressed using the polar coordinates r and θ so that

$$r_b = r_b(\theta, t). \tag{2.8}$$

Substituting (2.7), (2.8) into (2.4) and equating to zero the singular and regular parts in the resulting equations we obtain

$$\frac{\partial q}{\partial t} + (u - \dot{X})\frac{\partial q}{\partial x} + (v - \dot{Y})\frac{\partial q}{\partial y} + \frac{\beta}{h}\left[(y + Y)\left(\frac{\partial u}{\partial x} + \frac{\partial v}{\partial y}\right) + v\right] = 0, \tag{2.9a}$$

$$\frac{\partial r_b}{\partial t} + \frac{V^*|_b}{r_b}\frac{\partial r_b}{\partial \theta} - U^*|_b = 0, \tag{2.9b}$$

where $U^* = U - \dot{X}\cos\theta - \dot{Y}\sin\theta$, $V^* = V + \dot{X}\sin\theta - \dot{Y}\cos\theta$ and $a|_b = a(r_b, \theta, t)$.

Since the patch boundary is a material line the total mass inside the patch is conserved in time,

$$\int_S h\,\mathrm{d}x\,\mathrm{d}y = \int_0^{2\pi} \mathrm{d}\theta \int_0^{r_b} rh\,\mathrm{d}r = M_0 = \text{constant}, \tag{2.10}$$

where S is the patch region bounded by the curve (2.8). Formally the conservation law (2.10) is obtained using (2.8), (2.9*b*) and the continuity equation (2.1*c*).

The location (x_C, y_C) of the centroid of the vortex patch is given by

$$(x_C, y_C) = \frac{1}{M_0}\int_S (x, y) h\,\mathrm{d}x\,\mathrm{d}y, \tag{2.11}$$

and we identify the vortex centre (and correspondingly the origin of the moving coordinate frame) with the patch centroid. By this definition the centroid is stationary in the moving coordinates and $(x_C, y_C) = 0$ whence by virtue of (2.11) we have

$$\int_0^{2\pi} \mathrm{d}\theta \int_0^{r_b} r^2 h \mathrm{e}^{\mathrm{i}\theta}\,\mathrm{d}r = 0. \tag{2.12}$$

Equations (2.1*a, b*), (2.7), (2.9*a, b*) and (2.12) form a closed system which allows us to calculate the vortex evolution and propagation.

https://doi.org/10.1017/S0022112001005468 Published online by Cambridge University Press

2.3. *Intense vortex*

Next we introduce the following non-dimensional variables:

$$\left.\begin{aligned}&(\bar{x},\bar{y})=\frac{1}{R_d}(x,y),\quad \bar{t}=f_0t,\quad (\bar{U},\bar{V})=\frac{(U,V)}{R_dh_\infty Q},\quad \bar{\hat{h}}=\frac{g'}{f_0R_d^2Qh_\infty}\hat{h},\\&\bar{q}=\frac{h_\infty}{\beta R_d}q,\quad \bar{r}_b=\frac{r_b}{R_d},\quad (\bar{\dot{X}},\bar{\dot{Y}})=\frac{(\dot{X},\dot{Y})}{\beta R_d^2}.\end{aligned}\right\}\tag{2.13}$$

Our scaling is based on the assumptions (usual for geophysical applications) that the vortex size is comparable with the Rossby deformation scale $R_d=\sqrt{g'h_\infty}/f_0$, and the Coriolis force and the pressure gradients are of the same order in the momentum equations (2.1*a*, *b*). Also we assume that the regular component of the potential vorticity q and the vortex propagation are initiated by the β-effect (see also Reznik & Dewar 1994); the 'fast' time scale f_0^{-1} is caused by the presence of inertia–gravity waves in the model.

Two non-dimensional parameters play an important role in this problem,

$$\varepsilon=\frac{U_p}{f_0R_d},\quad \varepsilon_\beta=\frac{\beta R_d}{f_0}=\frac{\beta R_d^2}{U_p}\varepsilon,\tag{2.14a, b}$$

where $U_p=R_dh_\infty Q$ is the typical orbital velocity. Here ε is the Rossby number, and ε_β is the ratio of a typical Rossby wave frequency to the inertial frequency f_0. We assume the vortex to be intense, i.e. its orbital velocity U_p greatly exceeds the typical translation speed βR_d^2. Thus

$$\varepsilon_\beta\ll\varepsilon.\tag{2.15}$$

For typical oceanic parameters in midlatitudes, $\beta=2\times10^{-13}\,\mathrm{cm^{-1}\,s^{-1}}$, $R_d=50\,\mathrm{km}$, $f_0=10^{-4}\,\mathrm{s^{-1}}$, the parameter $\varepsilon_\beta=0.01$. To estimate the Rossby number we consider the initial axisymmetric vortex defined by (2.6). In non-dimensional form these equations are written as follows (bars and circumflexes are omitted):

$$\varepsilon\frac{V_I^2}{r}+V_I=\frac{\mathrm{d}h_I}{\mathrm{d}r},\quad \frac{\zeta_I-h_I}{1+\varepsilon h_I}=\gamma H(r_I-r),\quad \zeta_I=\frac{\mathrm{d}V_I}{\mathrm{d}r}+\frac{V_I}{r}.\tag{2.16a–c}$$

The depth and velocity profiles for $\varepsilon=0.1$ are shown in figure 1 (see § 3 for more detailed discussion). The profiles depend only weakly on the Rossby number and the maximum orbital velocity is approximately 0.4, which corresponds to dimensional velocity $U_{pm}=0.4U_p$. To fit the model vortex to a vortex with maximum velocity U_p^* one should choose the vorticity amplitude in such a way that $U_{pm}=U_p^*$, i.e. $U_p=U_p^*/0.4$; therefore the Rossby number (2.14*a*) in our problem is

$$\varepsilon=\frac{U_p^*}{0.4f_0R_d}.\tag{2.17}$$

For mid-oceanic eddies $U_p^*=20\,\mathrm{cm\,s^{-1}}$ and so $\varepsilon=0.1$, while for rings $U_p^*=1\,\mathrm{m\,s^{-1}}$, and so then $\varepsilon=0.5$. In what follows we focus on the case of mid-oceanic eddies, and so we may put

$$\varepsilon\ll1,\quad \varepsilon_\beta=\varepsilon^2.\tag{2.18}$$

Note that in the case of rings the parameter ε_β is effectively the only small parameter in the model.

In non-dimensional variables the system (2.1*a*, *b*), (2.7), (2.9*a*, *b*) and (2.12) becomes,

https://doi.org/10.1017/S0022112001005468 Published online by Cambridge University Press

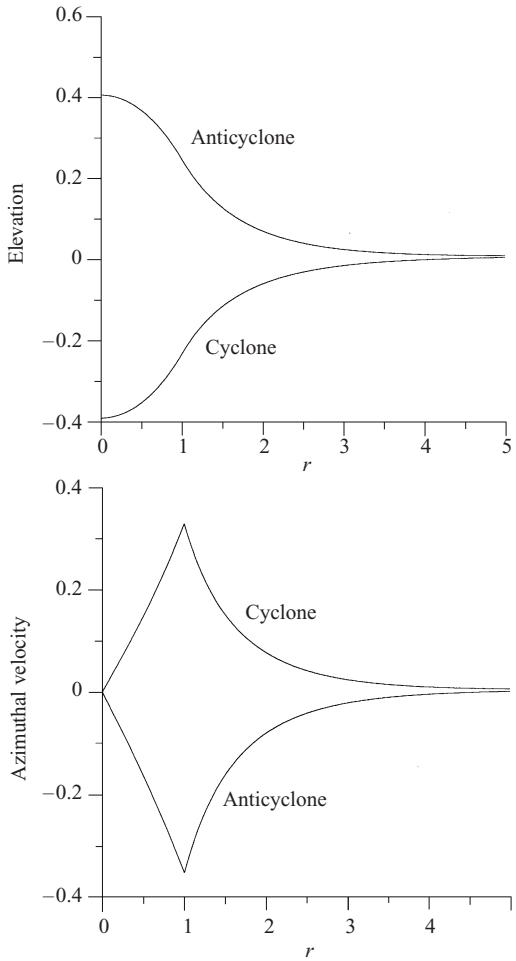


FIGURE 1. Radial profiles of the initial elevation $h_I(r)$ and the initial azimuthal velocity $V_I(r)$; $\varepsilon = 0.1$.

in polar coordinates,

$$\frac{\partial U}{\partial t} + \varepsilon\left[U^*\frac{\partial U}{\partial r} + \frac{V^*}{r}\left(\frac{\partial U}{\partial \theta} - V\right)\right] - [1 + \varepsilon^2(y + \varepsilon^2 Y)]V = -\frac{\partial h}{\partial r}, \tag{2.19a}$$

$$\frac{\partial V}{\partial t} + \varepsilon\left[U^*\frac{\partial V}{\partial r} + \frac{V^*}{r}\left(\frac{\partial V}{\partial \theta} + U\right)\right] + [1 + \varepsilon^2(y + \varepsilon^2 Y)]U = -\frac{1}{r}\frac{\partial h}{\partial \theta}, \tag{2.19b}$$

$$\frac{\partial q}{\partial t} + \varepsilon\left(U^*\frac{\partial q}{\partial r} + \frac{V^*}{r}\frac{\partial q}{\partial \theta}\right) + \frac{\varepsilon}{1 + \varepsilon h}[(y + \varepsilon^2 Y)\nabla \cdot \boldsymbol{U} + U\sin\theta + V\cos\theta] = 0, \tag{2.19c}$$

$$\frac{\zeta - h}{1 + \varepsilon h} = \gamma H(r_b - r) + \varepsilon q, \quad \zeta = \frac{1}{r}\left[\frac{\partial}{\partial r}(rV) - \frac{\partial U}{\partial \theta}\right], \tag{2.19d}$$

$$\frac{\partial r_b}{\partial t} + \varepsilon\left(\frac{V^*|_b}{r_b}\frac{\partial r_b}{\partial \theta} - U^*|_b\right) = 0, \tag{2.19e}$$

https://doi.org/10.1017/S0022112001005468 Published online by Cambridge University Press

$$\int_0^{2\pi} \mathrm{d}\theta \int_0^{r_b} r^2(1+\varepsilon h)\mathrm{e}^{\mathrm{i}\theta}\,\mathrm{d}r = 0, \tag{2.19f}$$

$$[U] = [V] = [h] = [\nabla h] = 0. \tag{2.19g}$$

Here the bars have been omitted, and

$$U^* = U - \varepsilon(\dot{X}\cos\theta + \dot{Y}\sin\theta), \quad V^* = V + \varepsilon(\dot{X}\sin\theta - \dot{Y}\cos\theta), \tag{2.20a}$$

$$[a] = a(r_b - 0, \theta, t) - a(r_b + 0, \theta, t), \tag{2.20b}$$

$$\nabla \cdot \boldsymbol{U} = \frac{\partial U}{\partial r} + \frac{U}{r} + \frac{1}{r}\frac{\partial V}{\partial \theta}. \tag{2.20c}$$

When deriving (2.19*f*) from (2.12) we use the relation $\hat{h}/h_\infty = O(\varepsilon)$ which follows from (2.13), (2.14). The conditions (2.19*g*) state the continuity at the patch boundary $r = r_b(\theta, t)$ of the velocity, pressure, and pressure gradient fields. The initial conditions to the system (2.19) are

$$q = 0, \quad V = V_I(r), \quad U = 0, \quad h = h_I(r) \quad \text{for} \quad t = 0, \tag{2.21}$$

where V_I, h_I are found from (2.16).

This system of equations generalizes to the shallow-water case the quasi-geostrophic a model of a vortex with piecewise-constant potential vorticity suggested by Sutyrin & Flierl (1994), and developed in RGB.

2.4. *Asymptotic expansions*

A solution to the system (2.19*a–g*) is sought in the form of the following asymptotic expansions:

$$U = \varepsilon U_1(r, \theta, t, T_1, T_2, \ldots) + \cdots, \tag{2.22a}$$

$$V = V_I(r) + \varepsilon V_I(r, \theta, t, T_1, T_2, \ldots) + \cdots, \tag{2.22b}$$

$$h = h_I(r) + \varepsilon h_1(r, \theta, t, T_1, T_2, \ldots) + \cdots, \tag{2.22c}$$

$$q = q_0(r, \theta, t, T_1, T_2, \ldots) + \varepsilon q_1(r, \theta, t, T_1, T_2, \ldots) + \cdots, \tag{2.22d}$$

$$r_b = r_I + \varepsilon r_1(\theta, t, T_1, T_2, \ldots) + \cdots, \tag{2.22e}$$

$$(X, Y) = (X_0, Y_0)(t, T_1, T_2, \ldots) + \varepsilon(X_1, Y_1)(t, T_1, T_2, \ldots) + \cdots. \tag{2.22f}$$

The initial vortex fields V_I, h_I are also represented in the same form:

$$V_I = V_{I0}(r) + \varepsilon V_{I1}(r) + \cdots, \tag{2.23a}$$

$$h_I = h_{I0}(r) + \varepsilon h_{I1}(r) + \cdots, \tag{2.23b}$$

$$U_I = 0, \quad r_I = 1. \tag{2.23c}$$

The slow times $T_n = \varepsilon^n t, n = 1, 2, \ldots$, are related to typical swirling times due to successive terms in the asymptotic expansion of the initial vortex field V_I, h_I. These are needed to prevent the regular vorticity q from a secular growth in time.

Since we are intending to examine development of the initial vortex V_I, h_I, all correction fields in (2.22) should satisfy a zero initial condition:

$$V_{m+1} = h_{m+1} = r_{m+1} = q_m = X_m = Y_m = 0 \quad \text{for} \quad t = 0, \quad m = 0, 1, 2, \ldots. \tag{2.24}$$

The simplest formal way to derive the equations for the unsteady fields in (2.22) consists of three steps: (i) substitution of (2.23) into (2.16) to obtain the nth-order initial field correction; (ii) substitution of (2.22), (2.23) into (2.19) to obtain the

https://doi.org/10.1017/S0022112001005468 Published online by Cambridge University Press

nth-order correction for the 'composite' field (e.g. $V_{In}(r) + V_n(r, \theta, t, T_1, T_2, \ldots)$); (iii) subtraction of the equations for the nth-order initial field from the corresponding equations for the same order 'composite' field to obtain the desired equations.

Note that the expansions (2.22) are regular in the spatial coordinates, contrary to the purely barotropic case with infinite Rossby scale where the far-field solution depends on the stretched coordinates $(x_s, y_s) = \varepsilon(x, y)$. In that case, it is necessary to match the near- and far-field asymptotic expansions in order to obtain a uniformly valid solution (see Reznik & Dewar 1994; Llewellyn Smith 1997 for details). In the case under consideration the Rossby scale is finite, and, correspondingly, the group velocity of Rossby waves is bounded in absolute value. Indeed, more precisely, the Rossby wave group velocity is $O(\varepsilon)$ for all wavelengths, and hence even on the long time scale T the Rossby waves remain in the vortex vicinity. Hence, at least up to times of $O(\varepsilon)$, there is no need to treat the Rossby wave far field separately.

Another possible source of the far-field irregularity is due to the fast inertia–gravity waves radiated by the vortex. The phase and group velocities of these waves greatly exceed both the typical swirling speed U_p (for small Rossby number ε) and the phase and group velocities of the Rossby waves. Therefore these waves excite the far-field motion practically instantaneously in comparison with the typical Rossby time scale $T_w = (\beta R)^{-1}$ and the advective time scale $T_d = R_d/U_p$. However, the analysis shows (see below and also Reznik, Zeitlin & Ben Jelloul 2001) that there is no need to introduce expansions of a special form to describe the far field of inertia–gravity waves, at least in the lowest order. The slow evolution of the vortex does not lead to radiation of the fast waves, except for the aforementioned initial rapid transient adjustment, and these waves cannot be captured by the weak vortex flow. Thus, the lowest-order inertia–gravity waves do not interact with the slow vortex and are described by the homogeneous linear wave equation throughout the whole plane (see §§ 4, 5 below).

3. Initial state

Using equations (2.16) and the expansions (2.23) one can readily find the initial state V_I, h_I to any desired level of accuracy. The lowest-order quantities are given by

$$h_{I0} = \gamma \begin{cases} -1 + K_1(1)I_0(r), & r \leqslant 1 \\ -I_1(1)K_0(r), & r > 1, \end{cases} \quad V_{I0} = \gamma \begin{cases} K_1(1)I_1(r), & r \leqslant 1 \\ I_1(1)K_1(r), & r > 1, \end{cases} \tag{3.1a,b}$$

and are identical to the initial geostrophic streamfunction and azimuthal velocity in RGB (see equations (5.2) to (5.4) there). The functions $K_m(r), I_m(r)$, $m = 0, 1, 2, \ldots$, are the modified Bessel functions of mth order, therefore V_{I0}, h_{I0} and all other fields decay exponentially for $r \to \infty$.

In the first-order approximation we have

$$h_{I1} = s_1 + s_2, \quad V_{I1} = \frac{\mathrm{d}h_{I1}}{\mathrm{d}r} - \frac{V_{I0}^2}{r} \tag{3.2a,b}$$

where

$$s_1 = -I_0(r) \int_r^\infty K_1(z) V_{I0}^2 \, \mathrm{d}z + K_0(r) \int_0^r I_1(z) V_{I0}^2 \, \mathrm{d}z, \tag{3.3a}$$

$$s_2 = \gamma \begin{cases} -I_0(r) \displaystyle\int_r^1 z K_0(z) h_{I0} \, \mathrm{d}z - K_0(r) \int_0^r z I_0(z) h_{I0} \, \mathrm{d}z, & r \leqslant 1 \\ -K_0(r) \displaystyle\int_0^1 z I_0(z) h_{I0} \, \mathrm{d}z, & r > 1. \end{cases} \tag{3.3b}$$

https://doi.org/10.1017/S0022112001005468 Published online by Cambridge University Press

The second-order correction to the initial vortex can be written as

$$h_{I2} = a_1 + a_2, \quad V_{I2} = \frac{\mathrm{d}h_{I2}}{\mathrm{d}r} - 2\frac{V_{I0}V_{I1}}{r}, \tag{3.4a,b}$$

$$a_1 = 2\left[-I_0(r)\int_r^\infty K_1(z)V_{I0}V_{I1}\,\mathrm{d}z + K_0(r)\int_0^r I_1(z)V_{I0}V_{I1}\,\mathrm{d}z\right], \tag{3.5a}$$

$$a_2 = \gamma\begin{cases} -I_0(r)\displaystyle\int_r^1 zK_0(z)h_{I1}\,\mathrm{d}z - K_0(r)\int_0^r zI_0(z)h_{I1}\,\mathrm{d}z, & r \leqslant 1 \\ -K_0(r)\displaystyle\int_0^1 zI_0(z)h_{I1}\,\mathrm{d}z, & r > 1. \end{cases} \tag{3.5b}$$

The elevation and azimuthal velocity profiles $h_I(r), V_I(r)$ are shown in figure 1 for $\varepsilon = 0.1$. They are similar to corresponding profiles of real geophysical eddies, for example oceanic rings. The elevation h_I in the vortex centre is maximum for the anticyclone and minimum for the cyclone, and decays monotonically in absolute value when moving to the vortex periphery. The azimuthal velocity V_I is positive for the cyclone and negative for the anticyclone, and grows in absolute value from zero at the vortex centre to the maximum value reached at the patch boundary; it decays with further increasing distance from the vortex centre. An interesting feature is that the anticyclone is somewhat more intense than the cyclone for the same vorticity amplitude; obviously this effect is related to ageostrophic terms in (2.16*a*, *b*).

4. Algorithm

In this Section we outline the algorithm used to derive the nth approximation in the expansions (2.22). Substitution of (2.22), (2.23) into the governing system (2.19) gives the following problem at the nth order:

$$\frac{\partial U_n}{\partial t} - V_n = -\frac{\partial h_n}{\partial r} + F(U)_n, \quad \frac{\partial V_n}{\partial t} + U_n = -\frac{1}{r}\frac{\partial h_n}{\partial \theta} + F(V)_n, \tag{4.1a,b}$$

$$\frac{\partial q_n}{\partial t} + \frac{\partial q_{n-1}}{\partial T_1} + \Omega_0\frac{\partial q_{n-1}}{\partial \theta} = F(q)_n, \tag{4.1c}$$

$$\zeta_n - h_n = q_{n-1} + F(\zeta)_n, \quad \zeta_n = \frac{1}{r}\left[\frac{\partial}{\partial r}(rV_n) - \frac{\partial U_n}{\partial \theta}\right], \tag{4.1d,e}$$

$$\frac{\partial r_{n+1}}{\partial t} + \frac{\partial r_n}{\partial T_1} + \Omega_0(1)\frac{\partial r_n}{\partial \theta} - U_n|_b + \dot{X}_{n-1}\cos\theta + \dot{Y}_{n-1}\sin\theta = F(r)_n, \tag{4.1f}$$

$$\int_0^{2\pi} \mathrm{e}^{\mathrm{i}\theta}\mathrm{d}\theta \int_0^1 r^2 h_n \mathrm{d}r + \int_0^{2\pi}(h_{I0}|_b r_n + r_{n+1})\mathrm{e}^{\mathrm{i}\theta}\mathrm{d}\theta = F(B)_n, \tag{4.1g}$$

$$[U_n] = D(U)_n, \quad [h_n] = D(h)_n, \quad [V_n] = -[V_{I0}']r_n + D(V)_n, \quad \left[\frac{\partial h_n}{\partial r}\right] = -[V_{I0}']r_n + D(h')_n. \tag{4.1h}$$

The functions $F(U)_n$, $D(U)_n$ etc. in (4.1) are known from the preceding approximations; $\Omega_0 = \Omega_0(r) = V_{I0}/r$ is the lowest-order angular velocity of the initial vortex; here and below $a|_b = a(1, \theta, t)$, $[a] = a(1-0, \theta, t) - a(1+0, \theta, t)$.

It is convenient to represent each quantity in (4.1) as a sum of the fast and slow components, i.e.

$$a = \bar{a} + \tilde{a}, \quad \bar{a} = \langle a \rangle, \tag{4.2}$$

https://doi.org/10.1017/S0022112001005468 Published online by Cambridge University Press

where the slow component $\bar{a}$ is derived by averaging of a with respect to the fast time t,

$$\langle a\rangle = \lim_{\bar{T}\to\infty}\frac{1}{\bar{T}}\int_0^{\bar{T}} a\,\mathrm{d}t. \tag{4.3}$$

An important point is that some information about the variables r_n, q_{n-1} is obtained at the preceding $(n-1)$th step: we know the fast components $\tilde{r}_n, \tilde{q}_{n-1}$, and the first azimuthal component $\bar{R}_n^{(1)}$ of the slow component $\bar{r}_n$, where

$$\bar{R}_n^{(1)} = \frac{\mathrm{i}}{\pi}\int_0^{2\pi}\bar{r}_n \mathrm{e}^{-\mathrm{i}\theta}\mathrm{d}\theta. \tag{4.4}$$

We will show that analysis of the system (4.1) given $\tilde{r}_n, \tilde{q}_{n-1}, \bar{R}_n^{(1)}$ allows us to determine the nth-order fields and the quantities $\tilde{r}_{n+1}, \tilde{q}_n, \bar{R}_{n+1}^{(1)}$, i.e. the algorithm is self-consistent.

4.1. *Analysis of slow fields*

Applying the averaging operator (4.3) to the system (4.1) gives the equations for the slow components,

$$\bar{V}_n = \frac{\partial\bar{h}_n}{\partial r} - \bar{F}(U)_n, \quad \bar{U}_n = -\frac{1}{r}\frac{\partial\bar{h}_n}{\partial\theta} + \bar{F}(V)_n, \tag{4.5a,b}$$

$$\frac{\partial\bar{q}_{n-1}}{\partial T_1} + \Omega_0\frac{\partial\bar{q}_{n-1}}{\partial\theta} = \bar{F}(q)_n, \tag{4.5c}$$

$$\bar{\zeta}_n - \bar{h}_n = \bar{q}_{n-1} + \bar{F}(\zeta)_n, \quad \bar{\zeta}_n = \frac{1}{r}\left[\frac{\partial}{\partial r}(r\bar{V}_n) - \frac{\partial\bar{U}_n}{\partial\theta}\right], \tag{4.5d,e}$$

$$\frac{\partial\bar{r}_n}{\partial T_1} + \Omega_0(1)\frac{\partial\bar{r}_n}{\partial\theta} - \bar{U}_n|_b + \bar{\dot{X}}_{n-1}\cos\theta + \bar{\dot{Y}}_{n-1}\sin\theta = \bar{F}(r)_n, \tag{4.5f}$$

$$\int_0^{2\pi}\mathrm{e}^{\mathrm{i}\theta}\mathrm{d}\theta\int_0^1 r^2\bar{h}_n\mathrm{d}r + \int_0^{2\pi}(h_{I0}|_b\bar{r}_n + \bar{r}_{n+1})\mathrm{e}^{\mathrm{i}\theta}\mathrm{d}\theta = \bar{F}(B)_n, \tag{4.5g}$$

$$[\bar{U}_n] = \bar{D}(U)_n, \quad [\bar{h}_n] = \bar{D}(h)_n, \quad [\bar{V}_n] = -[V_{I0}']\bar{r}_n + \bar{D}(V)_n, \quad \left[\frac{\partial\bar{h}_n}{\partial r}\right] = -[V_{I0}']\bar{r}_n + \bar{D}(h')_n. \tag{4.5h–k}$$

Equations (4.4), (4.5) form a closed system for the determination of the slow components. First we analyse (4.5c) for the vorticity correction $\bar{q}_{n-1}$. Then we reduce (4.5a,b), (4.5d,e) to one equation for the slow elevation $\bar{h}_n$:

$$\nabla^2\bar{h}_n - \bar{h} = \bar{F}(h)_n, \quad \bar{F}(h)_n = \bar{q}_{n-1} + \bar{F}(\zeta)_n + \frac{1}{r}\left[\frac{\partial}{\partial r}(r\bar{F}(U)_n) + \frac{\partial\bar{F}(V)_n}{\partial\theta}\right]. \tag{4.6}$$

Equations (4.6), (4.5f), (4.4) and (4.5i,k) allow us to define $\bar{h}_n$ and $\bar{r}_n$. The function $\bar{h}_n$ is split into two components $\bar{h}_{n1}$, $\bar{h}_{n2}$:

$$\bar{h}_n = \bar{h}_{n1} + \bar{h}_{n2}, \tag{4.7a}$$

$$\nabla^2\bar{h}_{n1} - \bar{h}_{n1} = \bar{F}(h)_n, \quad [\bar{h}_{n1}] = \bar{D}(h)_n, \quad \left[\frac{\partial\bar{h}_{n1}}{\partial r}\right] = \bar{D}(h')_n, \tag{4.7b}$$

$$\nabla^2\bar{h}_{n2} - \bar{h}_{n2} = 0, \quad [\bar{h}_{n2}] = 0, \quad \left[\frac{\partial\bar{h}_{n2}}{\partial r}\right] = -[V_{I0}']\bar{r}_n. \tag{4.7c}$$

https://doi.org/10.1017/S0022112001005468 Published online by Cambridge University Press

The component $\bar{h}_{n1}$ is determined from (4.7*b*) in a unique way given $\bar{F}(h)_n$, $\bar{D}(h)_n$, $\bar{D}(h')_n$. The component $\bar{h}_{n2}$ and the boundary perturbation $\bar{r}_n$ are decomposed into Fourier series in θ:

$$\bar{r}_n = \sum_{m=0}^{\infty} \mathrm{Im}(\bar{R}_n^{(m)} \mathrm{e}^{\mathrm{i}n\theta}), \quad \bar{h}_{n2} = -\gamma \sum_{m=0}^{\infty} \Phi_m \, \mathrm{Im}(\bar{R}_n^{(m)} \mathrm{e}^{\mathrm{i}m\theta}). \tag{4.8a, b}$$

Here

$$\bar{R}_n^{(m)} = \frac{\mathrm{i}}{\pi} \int_0^{2\pi} \bar{r}_n \mathrm{e}^{-\mathrm{i}m\theta} \mathrm{d}\theta, \quad \Phi_m = \begin{cases} K_m(1) I_m(r), & r \leqslant 1 \\ I_m(1) K_m(r), & r > 1. \end{cases} \tag{4.9a, b}$$

Expressing $\bar{U}_n$ in (4.5*f*) in terms of $\bar{h}_n$ (see (4.5*b*)) and substituting the Fourier series (4.8*a*, *b*) into the resulting equation we find the slow translation speed components $\bar{\dot{X}}_{n-1}$, $\bar{\dot{Y}}_{n-1}$ and the remaining Fourier components of $\bar{r}_n$ (recall that $\bar{R}_n^{(1)}$ is known from the preceding $(n-1)$th step):

$$\bar{\dot{X}}_{n-1} + \mathrm{i}\bar{\dot{Y}}_{n-1} = -\mathrm{i}\frac{\partial \bar{R}_n^{(1)*}}{\partial T_1} + \mathrm{i}\bar{G}_n^{(1)*}, \tag{4.10}$$

$$\bar{R}_n^{(k)} = \bar{R}_n^{(k)}(\theta, 0)\mathrm{e}^{-\mathrm{i}\hat{\Omega}_k T_1} + \mathrm{e}^{-\mathrm{i}\hat{\Omega}_k T_1} \int_0^{T_1} \bar{G}_n^{(k)} \mathrm{e}^{\mathrm{i}\hat{\Omega}_k T_1} \mathrm{d}T_1, \quad k \neq 1. \tag{4.11}$$

Here $\bar{G}_n^{(k)}$, $k = 0, 1, \ldots$, are the coefficients of the Fourier decomposition of the function $\bar{G}_n$,

$$\bar{G}_n = \bar{F}(r)_n - \left(\frac{\partial \bar{h}_{n1}}{\partial \theta} - \bar{F}(V)_n \right) \Big|_b = \sum_{m=0}^{\infty} \mathrm{Im}(\bar{G}_n^{(m)} \mathrm{e}^{\mathrm{i}m\theta}), \quad \hat{\Omega}_m = \gamma m[\Phi_1(1) - \Phi_m(1)], \tag{4.12a, b}$$

and asterisks denotes the complex conjugate value.

Note that the initial conditions $\bar{R}_n^{(k)}(\theta, 0)$ follow from (2.24) given $\tilde{r}_n$. Knowing $\bar{r}_n$ we determine the component $\bar{h}_{n2}$ from (4.8*a*), and then the slow velocity components $\bar{U}_n$, $\bar{V}_n$ from (4.5*a*, *b*). Finally, we find the first azimuthal component $\bar{R}_{n+1}^{(1)}$ of the slow component $\bar{r}_{n+1}$ from (4.5*g*):

$$\bar{R}_{n+1}^{(1)} = \frac{\mathrm{i}}{\pi} \int_0^{2\pi} \bar{r}_{n+1} \mathrm{e}^{-\mathrm{i}\theta} \mathrm{d}\theta = \frac{\mathrm{i}}{\pi} \left(\bar{F}(B)_n^* - \int_0^{2\pi} \mathrm{e}^{-\mathrm{i}\theta} \mathrm{d}\theta \int_0^1 r^2 \bar{h}_n \mathrm{d}r \right) - h_{I0}|_b \bar{R}_n^{(1)}. \tag{4.13}$$

4.2. *Analysis of fast fields*

The equations for the fast components have the form

$$\frac{\partial \tilde{U}_n}{\partial t} - \tilde{V}_n = -\frac{\partial \tilde{h}_n}{\partial r} + \tilde{F}(U)_n, \quad \frac{\partial \tilde{V}_n}{\partial t} + \tilde{U}_n = -\frac{1}{r}\frac{\partial \tilde{h}_n}{\partial \theta} + \tilde{F}(V)_n, \tag{4.14a, b}$$

$$\frac{\partial \tilde{q}_n}{\partial t} + \frac{\partial \tilde{q}_{n-1}}{\partial T_1} + \Omega_0 \frac{\partial \tilde{q}_{n-1}}{\partial \theta} = \tilde{F}(q)_n, \tag{4.14c}$$

$$\tilde{\zeta}_n - \tilde{h}_n = \tilde{q}_{n-1} + \tilde{F}(\zeta)_n, \quad \tilde{\zeta}_n = \frac{1}{r}\left[\frac{\partial}{\partial r}(r\tilde{V}_n) - \frac{\partial \tilde{U}_n}{\partial \theta} \right] \tag{4.14d, e}$$

$$\frac{\partial \tilde{r}_{n+1}}{\partial t} + \frac{\partial \tilde{r}_n}{\partial T_1} + \Omega_0(1)\frac{\partial \tilde{r}_n}{\partial \theta} - \tilde{U}_n|_b + \tilde{\dot{X}}_{n-1}\cos\theta + \tilde{\dot{Y}}_{n-1}\sin\theta = \tilde{F}(r)_n, \tag{4.14f}$$

$$\int_0^{2\pi} \mathrm{e}^{\mathrm{i}\theta} \mathrm{d}\theta \int_0^1 r^2 \tilde{h}_n \mathrm{d}r + \int_0^{2\pi} (h_{I0}|_b \tilde{r}_n + \tilde{r}_{n+1}) \mathrm{e}^{\mathrm{i}\theta} \mathrm{d}\theta = \tilde{F}(B)_n, \tag{4.14g}$$

https://doi.org/10.1017/S0022112001005468 Published online by Cambridge University Press

$$[\tilde{U}_n] = \tilde{D}(U)_n, \quad [\tilde{h}_n] = \tilde{D}(h)_n, \quad [\tilde{V}_n] = -[V_{I0}']\tilde{r}_n + \tilde{D}(V)_n, \quad \left[\frac{\partial \tilde{h}_n}{\partial r}\right] = -[V_{I0}']\tilde{r}_n + \tilde{D}(h')_n. \tag{4.14h–k}$$

Since $\tilde{q}_{n-1}$ is known one can find $\tilde{q}_n$ from (4.14c). Then (4.14a, b, d, e) are reduced to a single equation for $\tilde{h}_n$ using the equations for vorticity $\tilde{\zeta}_n$ and divergence $\tilde{D}_n = \nabla \cdot \bar{\boldsymbol{U}}_n$, $\tilde{\boldsymbol{U}}_n = (\tilde{U}_n, \tilde{V}_n)$, following from the momentum equations (4.14a, b),

$$\frac{\partial \tilde{\zeta}_n}{\partial t} + \tilde{D}_n = \mathrm{rot}_z \tilde{\boldsymbol{F}}(\boldsymbol{U})_n, \quad \frac{\partial \tilde{D}_n}{\partial t} - \tilde{\zeta}_n = -\nabla^2 \tilde{h}_n + \nabla \cdot \tilde{\boldsymbol{F}}(\boldsymbol{U})_n. \tag{4.15a, b}$$

Here

$$\tilde{\boldsymbol{F}}(\boldsymbol{U})_n = (\tilde{F}(U)_n, \tilde{F}(V)_n), \quad \mathrm{rot}_z \boldsymbol{A} = \frac{1}{r}\frac{\partial}{\partial r}(rA_\theta) - \frac{\partial A_r}{\partial \theta}, \quad \text{for} \quad \boldsymbol{A} = (A_r, A_\theta). \tag{4.16a, b}$$

The resulting equation for $\tilde{h}_n$, has the form

$$-\frac{\partial^2 \tilde{h}_n}{\partial t^2} + \nabla^2 \tilde{h}_n - \tilde{h}_n = \tilde{F}(h)_n, \tag{4.17a}$$

$$\tilde{F}_{h_n} = \frac{\partial^2 (\tilde{q}_{n-1} + \tilde{F}(\zeta)_n)}{\partial t^2} + \tilde{q}_{n-1} + \tilde{F}(\zeta)_n + \nabla \cdot \tilde{\boldsymbol{F}}(\boldsymbol{U})_n - \frac{\partial}{\partial t}(\mathrm{rot}_z \tilde{\boldsymbol{F}}(\boldsymbol{U})_n). \tag{4.17b}$$

The conditions (4.14i, k) for $\tilde{h}_n$ are determined given $\tilde{r}_n$. One initial condition for $\tilde{h}_n$ is derived from (2.24) given the slow component $\bar{h}_n$,

$$\tilde{h}_n|_{t=0} = -\bar{h}_n|_{t=0}. \tag{4.18}$$

Another initial condition follows from (4.15a), (4.14d) and (2.24),

$$\left.\frac{\partial \tilde{h}_n}{\partial t}\right|_{t=0} = \nabla \cdot \bar{\boldsymbol{U}}_n|_{t=0} - \left[\frac{\partial (\tilde{q}_{n-1} + \tilde{F}(\zeta)_n)}{\partial t} - \mathrm{rot}_z \tilde{\boldsymbol{F}}(\boldsymbol{U})_n\right]_{t=0}. \tag{4.19}$$

Here $\bar{\boldsymbol{U}}_n = (\bar{U}_n, \bar{V}_n)$ is the known slow velocity. Equations (4.17), (4.18), (4.19) and (4.14i, k) form a closed system allowing us to calculate $\tilde{h}_n$. In turn, given $\tilde{h}_n$ one can find the fast velocity component $\tilde{\boldsymbol{U}}_n = (\tilde{U}_n, \tilde{V}_n)$ from (4.14a, b) and the first azimuthal component $\tilde{R}^{(1)}_{n+1}$ of $\tilde{r}_{n+1}$ using (4.14g). Knowing $\tilde{R}^{(1)}_{n+1}$, $\tilde{U}_n$ and $\tilde{r}_n$ one obtains the fast components of translation speed $\tilde{X}_{n-1}$, $\tilde{Y}_{n-1}$ and the other azimuthal components of $\tilde{r}_{n+1}$ from (4.14f). So the above analysis of the slow and fast components allows us to derive the nth-order fields given $\tilde{r}_n$, $\tilde{q}_{n-1}$ and $\bar{R}^{(1)}_n$ and the quantities $\tilde{r}_{n+1}$, $\tilde{q}_n$, $\bar{R}^{(1)}_{n+1}$ which are needed to calculate the next approximation.

The analysis starts from the simple equations

$$\tilde{q}_0 = \tilde{r}_1 = \tilde{R}^{(1)}_1 = 0 \tag{4.20}$$

which readily follow from (2.19c, e, f) in the lowest order. Using (4.20) we analyse the problem (4.1) for $n = 1$ and so on, following the algorithm described.

To study new physical effects we have to proceed up to the third-order approximation. Technically, it is not a problem to calculate the higher-order corrections using the above algorithm but the resulting formulae turn out to be very cumbersome. What is more important, many of them describe QG dynamics studied thoroughly in RGB. In the next Section we discuss briefly the most important formulae for the first and second corrections without a detailed derivation. More detail analysis of these corrections is given in Appendices A and B.

https://doi.org/10.1017/S0022112001005468 Published online by Cambridge University Press

5. Main results for the first- and second-order terms

5.1. *First-order correction: geostrophic β-gyres*

All first-order fields evolve slowly in time, and the fast components are absent in this approximation; that is, $\tilde{U}_1$, $\tilde{V}_1$, $\tilde{q}_1$, $\tilde{h}_1$ and $\tilde{r}_1$ are all zero (see Appendix A). Hence for these first-order variables we can omit the decomposition (4.2). The patch boundary perturbation is identically zero,

$$r_1 = 0, \tag{5.1}$$

so that the vortex patch shape still remains unchanged. All fields have a dipole structure, the regular vorticity q_0 being given by the equations

$$q_0 = q_{0s}\sin\theta + q_{0c}\cos\theta, \quad q_{0s} + \mathrm{i}q_{0c} = -r + (r + C_0)\mathrm{e}^{-\mathrm{i}\varphi_0} \tag{5.2a,b}$$

where

$$\varphi_0 = \Omega_0 T_1, \quad C_0 = C_0(r, T_2, \ldots), \quad C_0 = 0 \quad \text{for} \quad T_2 = 0. \tag{5.3}$$

The elevation field h_1 has a similar structure,

$$\nabla^2 h_1 - h_1 = q_0, \quad h_1 = A_{1s}\sin\theta + A_{1c}\cos\theta, \tag{5.4a,b}$$

the coefficients A_{1s}, A_{1c} being expressed in terms of the vorticity q_0,

$$A = A_{1s} + \mathrm{i}A_{1c} = -I_1(r)\int_r^\infty zK_1(z)Q_0\,\mathrm{d}z - K_1(r)\int_0^r zI_1(z)Q_0\,\mathrm{d}z, \tag{5.5a}$$

$$Q_0 = q_{0s} + \mathrm{i}q_{0c}. \tag{5.5b}$$

The first-order fields are geostrophically balanced, i.e. the velocities U_1, V_1 are related to the elevation h_1 by the geostrophic relations

$$U_1 = -\frac{1}{r}\frac{\partial h_1}{\partial\theta}, \quad V_1 = \frac{\partial h_1}{\partial r}. \tag{5.6a,b}$$

Finally, the lowest-order translation velocity is given by the formula

$$\dot{X}_0 + \mathrm{i}\dot{Y}_0 = -A^*(1, T_1, \ldots). \tag{5.7}$$

The solution (5.1), (5.2), (5.4), (5.5), (5.6) and (5.7) exactly coincides with the first-order solution in the quasi-geostrophic model of RGB. In other words, the first-order correction describes the slowly (in comparison with inertia–gravity waves) developing quasi-geostrophic β-gyres gradually increasing in magnitude, size and energy (see figure 2 and RGB). It is clearly seen from figure 2 that this process is accompanied by the rise of practically rectilinear uniform flow in the main vortex vicinity, intensifying and expanding with increasing time. Namely this flow advects the vortex with the translation speed (5.7) shown in figure 3 (see RGB for a further discussion of this and related issues).

The analysis given in RGB shows that the fields U_1, V_1, q_0 and the translation speed $(\dot{X}_0, \dot{Y}_0)$ are bounded for $T_1 \to \infty$. At the same time the spatial PV gradient associated with q_0 increases linearly with increasing time since $\partial q_0/\partial r = O(T_1)$ as seen from (5.2), (5.3). In other words, the asymptotic expansion for the PV gradient becomes disordered at times $t = O(\varepsilon^{-2})$ and the question arises about the range of time over which the expansions (2.22) remain a good approximation to the solution. To estimate this range we have considered the remainder arising when substituting the approximate solution $(U_I, V_I, h_I, r_I, 0) + \varepsilon(U_1, V_1, h_1, r_1, q_0)$ into the basic equations (2.19). Obviously,

https://doi.org/10.1017/S0022112001005468 Published online by Cambridge University Press

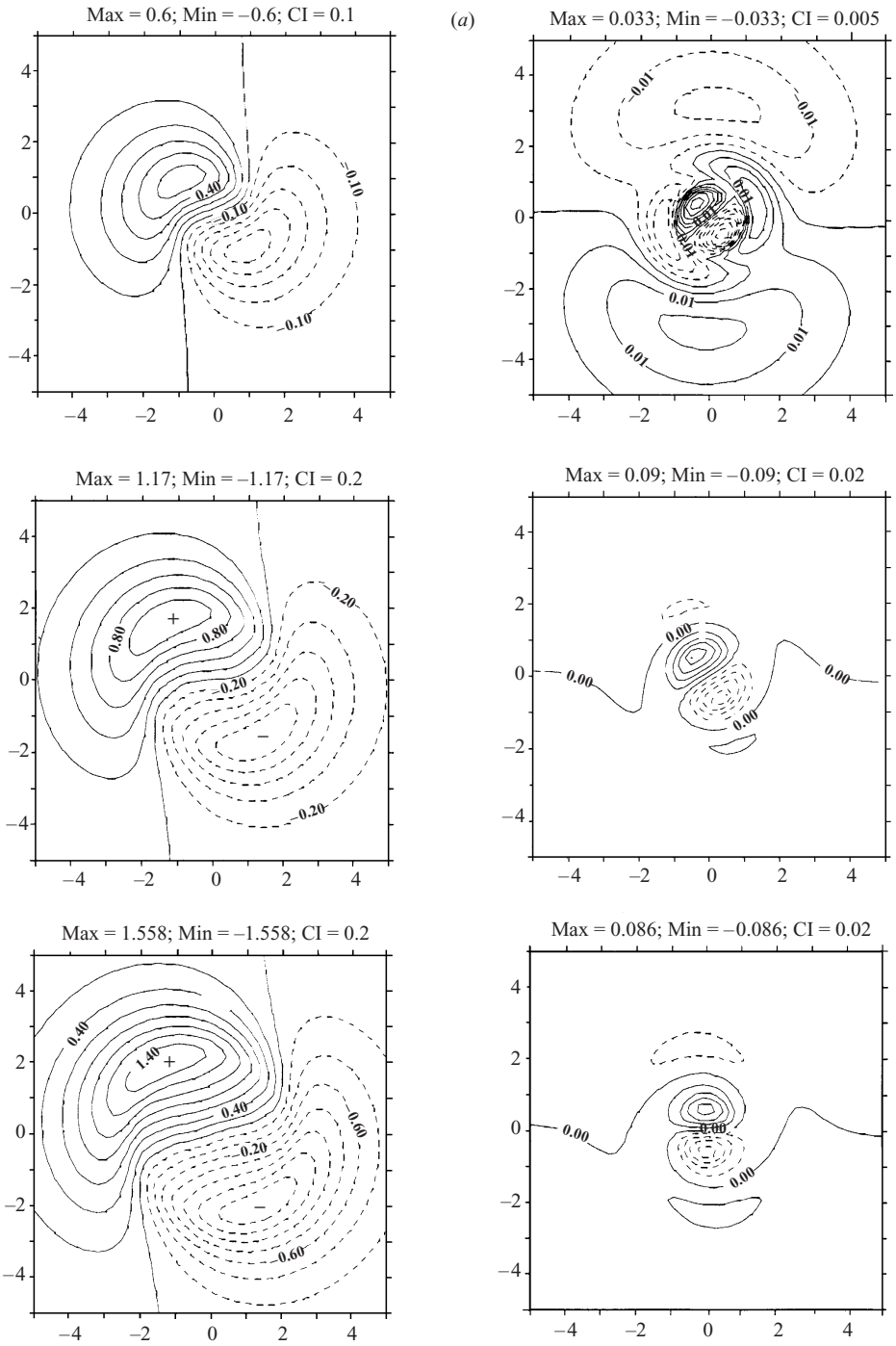


FIGURE 2. For caption see facing page.

the most 'dangerous' part of the remainder is related to the term $U^*\partial q/\partial r$ in (2.19c). The detailed analysis of this term is given in RGB (see §§ 5, 7 therein); here we note that the rapid growth of $\partial q/\partial r$ is compensated by the smallness of the residual flow U^* and the remainder remains small at least up to times $t = 1000 = O(\varepsilon^{-3})$. Thus the

https://doi.org/10.1017/S0022112001005468 Published online by Cambridge University Press

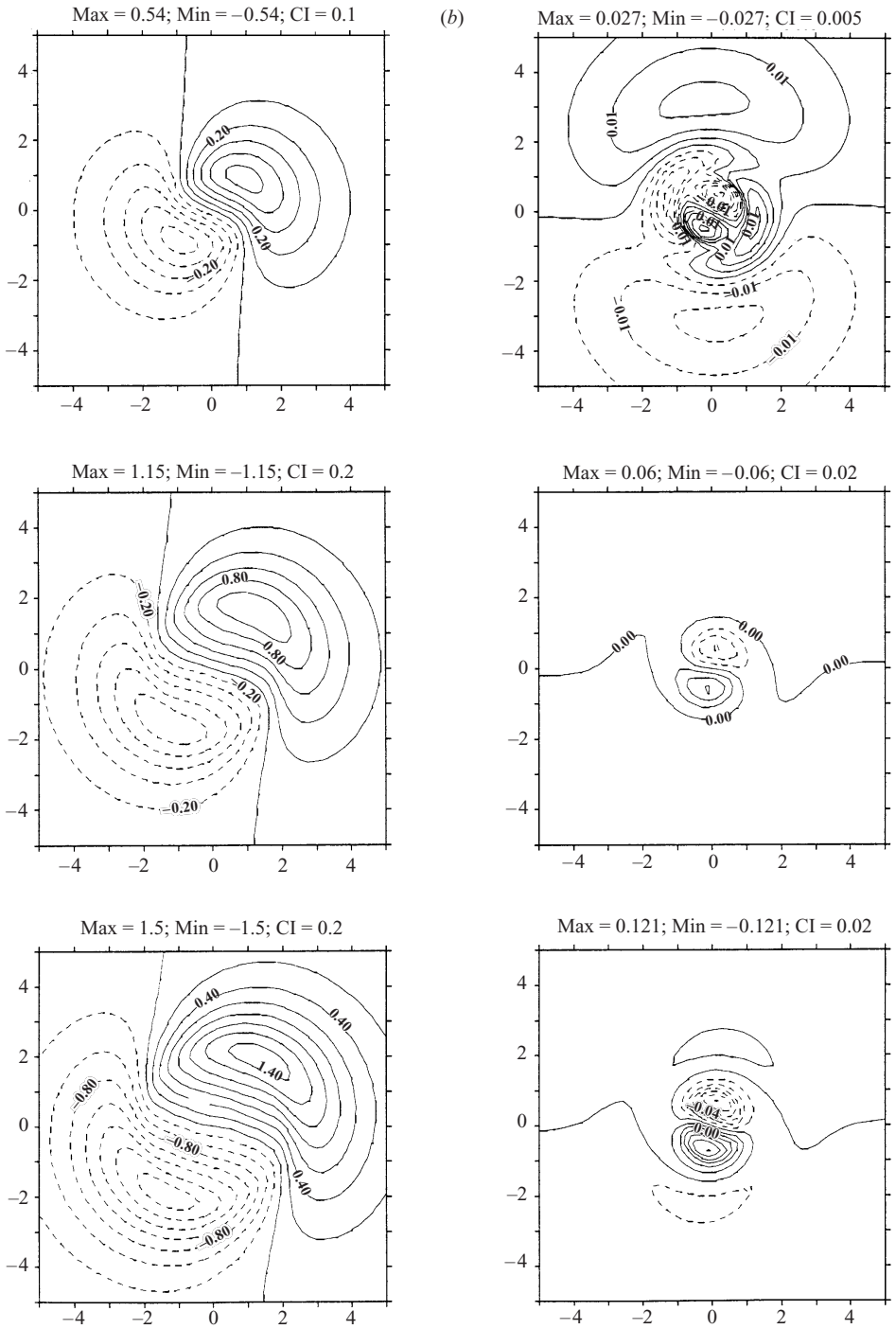


FIGURE 2. Development of the geostrophic β-gyre elevation $h_1(r, \theta, T_1, \ldots)$ (left) and the ageostrophic β-gyre elevation $\bar{h}_2^d(r, \theta, T_1, \ldots)$ (right). The upper figures correspond to $T_1 = 10$, middle to $T_1 = 50$, bottom to $T_1 = 100$. MAX and MIN are the maximum and minimum values of the fields shown; CI is the contour interval. (*a*) Anticyclone, (*b*) cyclone.

https://doi.org/10.1017/S0022112001005468 Published online by Cambridge University Press

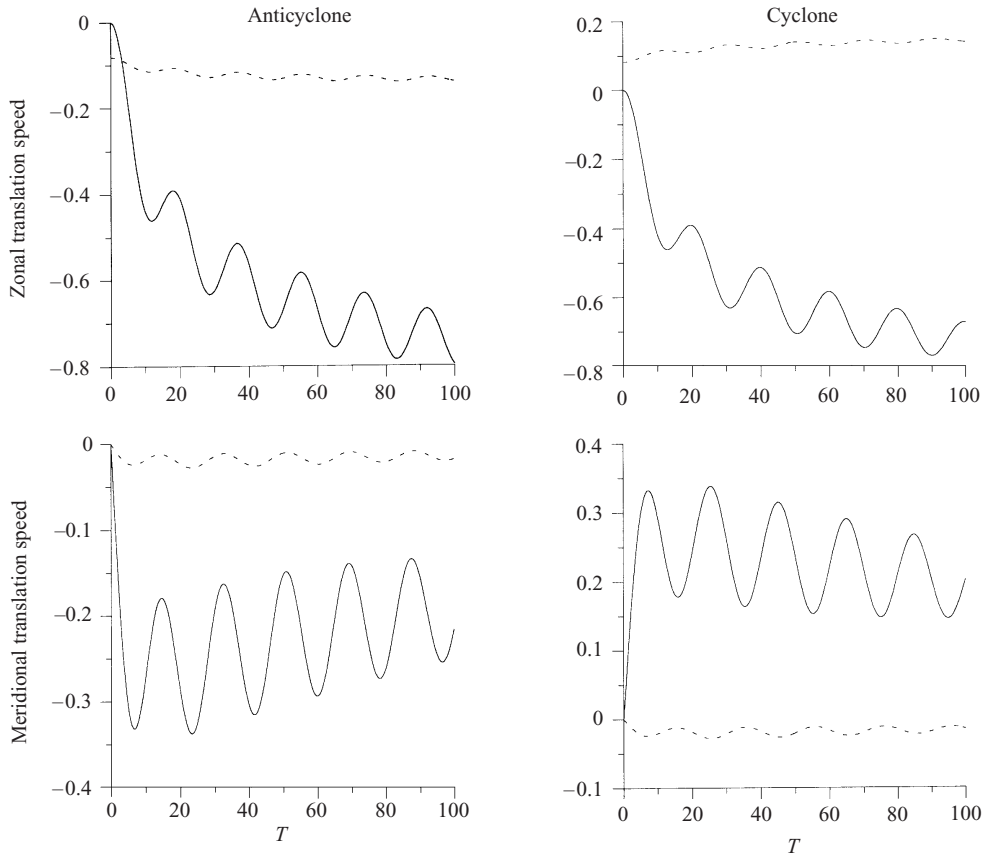


FIGURE 3. The translation speed components: solid lines – the lowest-order components induced by the geostrophic β-gyres; dashed lines – the corrections induced by the ageostrophic β-gyres. The time T coincides with the first slow time T_1.

disordering of the PV gradient does not prevent the expansions (2.22) from being a good approximation to the solution at times much longer than $t = O(\varepsilon^{-2})$.

Ageostrophic effects (the inertia–gravity wave radiation and a finite surface elevation) are absent in this level of approximation. To proceed to the next approximation the following equations are needed (see Appendix A for their derivation):

$$\tilde{r}_2 = 0, \quad \tilde{q}_1 = 0, \quad \bar{R}_2^{(1)} = -\int_0^1 r^2 A \, \mathrm{d}r. \tag{5.8a,b,c}$$

5.2. *Second-order fields and ageostrophic effects*

The second-order fields are more complicated than the first-order fields: (i) even their slow mode is not geostrophically balanced (the 'slow' functions $F(U)_2$, $F(V)_2$ are non-zero in (4.1a,b)); (ii) they contain both slow and fast modes; (iii) they possess the axisymmetric and quadrupole components as well as the dipole component.

The vorticity correction q_1 remains slow (see (5.8b)) and is given by

$$q_1 = -h_{10} q_0 + q_{12}, \tag{5.9}$$

where the term q_{12} is represented as a sum

$$q_{12} = q_{20}(r, T_1, \ldots) + q_{2s}(r, T_1, \ldots) \sin 2\theta + q_{2c}(r, T_1, \ldots) \cos 2\theta. \tag{5.10}$$

https://doi.org/10.1017/S0022112001005468 Published online by Cambridge University Press

Formulae for the functions q_{20}, q_{2s}, q_{2c} are given in Appendix B. The solution q_{12} exactly coincides with the second-order vorticity correction in the quasi-geostrophic model developed in RGB (cf. the solution (6.2), (6.3) therein). The axisymmetric term $q_{20}(r, T_1, \ldots)$ describes a decrease of the relative vorticity when the vortex travels along the meridian. The quadrupole term $q_{2s}\sin 2\theta + q_{2c}\cos 2\theta$ is induced by the nonlinear self-interaction of the first-order dipole circulation h_1, U_1, V_1.

The equations (4.7) for the slow elevation $\bar{h}_2$ become

$$\bar{h}_2 = \bar{h}_{21} + \bar{h}_{22}, \tag{5.11}$$

$$\nabla^2\bar{h}_{21} - \bar{h}_{21} = \gamma h_1 H(1-r) + \frac{1}{r}\left[2(V_{I0}V_1)' - 2V'_{I0}\frac{\partial U_1}{\partial\theta} + (r^2V_{I0})'\sin\theta\right] + q_{12}, \tag{5.12a}$$

$$[\bar{h}_{21}] = \left[\frac{\partial\bar{h}_{21}}{\partial r}\right] = 0, \tag{5.12b}$$

$$\nabla^2\bar{h}_{22} - \bar{h}_{22} = 0, \quad [\bar{h}_{22}] = 0, \quad \left[\frac{\partial\bar{h}_{22}}{\partial r}\right] = -[V'_{I0}]r_2. \tag{5.13}$$

We note that the function r_2 is non-zero and slow (as follows from (5.8*a*)).

The first two terms on the right-hand side of (5.12*a*) have a dipole structure, but the term q_{12} does not, as seen from (5.10). The solution to (5.12*a*, *b*) is conveniently represented as a sum

$$\bar{h}_{21} = \bar{h}^d_{21} + \bar{h}^c_{2g}, \tag{5.14}$$

where the dipole part $\bar{h}^d_{21}$ and non-dipole term $\bar{h}^c_{2g}$ satisfy the equations

$$\nabla^2\bar{h}^d_{21} - \bar{h}^d_{21} = \gamma h_1 H(1-r) + \frac{1}{r}\left[2(V_{I0}V_1)' - 2V'_{I0}\frac{\partial U_1}{\partial\theta} + (r^2V_{I0})'\sin\theta\right], \tag{5.15}$$

$$\nabla^2\bar{h}^c_{2g} - \bar{h}^c_{2g} = q_{12}, \tag{5.16}$$

respectively. The solution $\bar{h}^c_{2g}$ is written in the form

$$\bar{h}^c_{2g} = B_{20}(r, T_1, \ldots) + B_{2s}(r, T_1, \ldots)\sin 2\theta + B_{2c}(r, T_1, \ldots)\cos 2\theta. \tag{5.17}$$

The formulae for B_{20}, B_{2s}, B_{2c} are given in Appendix B. The solution (5.17) coincides with the continuous part of the second-order correction to the geostrophic stream function given by equations (6.4), (6.5) in RGB (without terms proportional to $R_2^{(2)}$). The axisymmetric part B_{20} is a correction to the main vortex profile induced by the β-effect, while the quadrupole term $B_{2s}\sin 2\theta + B_{2c}\cos 2\theta$ is initiated by the quadrupole terms in the vorticity correction (5.10).

The dipole part $\bar{h}^d_{21}$ is of the most interest here since it arises due to ageostrophic terms in the basic equations and causes the effects absent in QG models. The solution to (5.15) is conveniently represented in the form

$$\bar{h}^d_{21} = h^{(1)}_{21} + h^{(2)}_{21} + h^{(3)}_{21}, \quad h^{(k)}_{21} = \mathrm{Im}(E_k(r, T_1, \ldots)\mathrm{e}^{\mathrm{i}\theta}), \quad k = 1, 2, 3, \tag{5.18}$$

where

$$E_1 = \gamma\begin{cases} -I_1(r)\displaystyle\int_r^1 zK_1(z)A\,\mathrm{d}z - K_1(r)\int_0^r zI_1(z)A\,\mathrm{d}z, & r \leqslant 1 \\ -K_1(r)\displaystyle\int_0^1 zI_1(z)A\,\mathrm{d}z, & r > 1, \end{cases} \tag{5.19a}$$

https://doi.org/10.1017/S0022112001005468 Published online by Cambridge University Press

$$E_2 = 2\left[-I_1(r)\int_1^\infty K_2(z)\frac{V_{I0}}{z}(zA'-A)\,\mathrm{d}z + K_1(r)\int_0^r I_2(z)\frac{V_{I0}}{z}(zA'-A)\,\mathrm{d}z\right], \tag{5.19b}$$

$$E_3 = -I_1(r)\int_r^\infty zK_0(z)(zV_{I0}+h_{I0})\,\mathrm{d}z + K_1(r)\int_0^r zI_0(z)(zV_{I0}+h_{I0})\,\mathrm{d}z. \tag{5.19c}$$

Here A is defined by (5.5a). Knowing $\bar{h}_{21}^d$, $\bar{h}_{2g}^c$, and, consequently, $\bar{h}_{21}$ one can calculate the function $\bar{G}_2$ in (4.12a) for $n=2$ and determine the translation speed components $\bar{\dot{X}}_1$, $\bar{\dot{Y}}_1$ from (4.10) using $\bar{R}_2^{(1)}$ from (5.8c). As a result we have

$$\bar{\dot{Y}}_1 + \mathrm{i}\bar{\dot{X}}_1 = -\int_0^1 r^2\frac{\partial Q_0}{\partial T_1}\mathrm{d}r - \left.\frac{\partial A}{\partial T_1}\right|_b - \mathrm{i}\Omega_0(1)(A'-A)|_b - \mathrm{i}(E_1+E_2+E_3)|_b. \tag{5.20}$$

Note that only the dipole part $\bar{h}_{21}^d$ of $\bar{h}_{21}$ enters the function $\bar{G}_2^{(1)*}$ in (4.10) and causes the last term in (5.20) (which turns out to be most important; see the next Section).

Also, knowing $\bar{G}_2$ one can calculate the coefficients (4.9a) in the Fourier representation (4.8a) for r_2:

$$r_2 = \sum_{m=1}^{2}\mathrm{Im}(R_2^{(m)}\mathrm{e}^{\mathrm{i}m\theta}), \quad R_2^{(2)} = -2\mathrm{i}\mathrm{e}^{-\mathrm{i}\hat{\Omega}_2 T_1}\int_0^{T_1}(B_{2s}+\mathrm{i}B_{2c})|_b\mathrm{e}^{\mathrm{i}\hat{\Omega}_2 T_1}\mathrm{d}T_1, \tag{5.21a,b}$$

where the coefficient $R_2^{(1)}$ is defined by (5.8c). Note that there is no axisymmetric component in r_2 (see below in § 7). Equations (5.21) together with (4.8b) allow us to obtain the function $\bar{h}_{22}$,

$$\bar{h}_{22} = -\gamma\sum_{n=1}^{2}\Phi_n\mathrm{Im}(R_2^{(n)}\mathrm{e}^{\mathrm{i}n\theta}). \tag{5.22}$$

The slow elevation $\bar{h}_2$ is determined by (5.11), (5.14), (5.17), (5.18) and (5.22). The slow velocity corrections $\bar{U}_2$, $\bar{V}_2$ are given by (B 16a,b).

The fast corrections $\tilde{U}_2$, $\tilde{V}_2$, $\tilde{h}_2$ are solutions to the set of *homogeneous* equations,

$$\frac{\partial\tilde{U}_2}{\partial t} - \tilde{V}_2 = -\frac{\partial\tilde{h}_2}{\partial r}, \quad \frac{\partial\tilde{V}_2}{\partial t} + \tilde{U}_2 = -\frac{1}{r}\frac{\partial\tilde{h}_2}{\partial\theta}, \quad \tilde{\zeta}_2 - \tilde{h}_2 = 0, \tag{5.23a,b,c}$$

which can be reduced to the wave equation for $\tilde{h}_2$ with spatially localized initial conditions:

$$-\frac{\partial^2\tilde{h}_2}{\partial t^2} + \nabla^2\tilde{h}_2 - \tilde{h}_2 = 0, \quad \tilde{h}_2 = -\bar{h}_2, \quad \frac{\partial\tilde{h}_2}{\partial t} = -\frac{\partial\zeta_1}{\partial T_1} - V_{I0}\cos\theta \quad \text{for} \quad t=0. \tag{5.24a,b,c}$$

Simple analysis shows that both the initial fields (5.24b,c) and, therefore, the correction fields $\tilde{h}_2$, $\tilde{U}_2$, $\tilde{V}_2$ have a dipole structure,

$$\tilde{h}_2 = \tilde{h}_{2s}\sin\theta + \tilde{h}_{2c}\cos\theta, \quad (\tilde{U}_2,\tilde{V}_2) = (\tilde{U}_{2s},\tilde{V}_{2s})\sin\theta + (\tilde{U}_{2c},\tilde{V}_{2c})\cos\theta. \tag{5.25}$$

This results in a non-zero fast translation speed correction $\tilde{\dot{X}}_1$, $\tilde{\dot{Y}}_1$ given by equation (B 24) (see Appendix B for more details),

$$\tilde{\dot{Y}}_1 + \mathrm{i}\tilde{\dot{X}}_1 = \int_0^1 r^2\frac{\partial(\tilde{h}_{2s}+\mathrm{i}\tilde{h}_{2c})}{\partial t}\mathrm{d}r + (\tilde{U}_{2s}+\mathrm{i}\tilde{U}_{2c})|_b. \tag{5.26}$$

We emphasize that the translation speed correction $(\dot{X}_1, \dot{Y}_1)$ is absent in the QG model (see RGB) and is caused only by the ageostrophic effects.

https://doi.org/10.1017/S0022112001005468 Published online by Cambridge University Press

The system (5.24) describes the radiation of the dispersive fast inertia–gravity waves by the localized initial state (5.24*b*, *c*). The energy of these waves is conserved,

$$\int_0^{2\pi} \mathrm{d}\theta \int_0^{\infty} \left(\frac{\tilde{U}_2^2 + \tilde{V}_2^2}{2} + \frac{\tilde{h}_2^2}{2} \right) r \, \mathrm{d}r = \text{constant}, \tag{5.27}$$

which readily follows from (5.23). One can show also that the energy of interaction (E^{int}) between the fast waves and the lowest-order slow component is identically zero. In our case

$$E^{int} = \int_0^{2\pi} \mathrm{d}\theta \int_0^{\infty} (U_1 \tilde{U}_2 + V_1 \tilde{V}_2 + h_1 \tilde{h}_2) r \, \mathrm{d}r, \tag{5.28}$$

and taking into account (5.6), (5.23*c*) we have

$$E^{int} = \int_0^{2\pi} \mathrm{d}\theta \int_0^{\infty} h_1 (\tilde{h}_2 - \tilde{\zeta}_2) r \, \mathrm{d}r = 0. \tag{5.29}$$

Physically (5.27) and (5.29) mean that the lowest-order inertia–gravity wave field is energetically insignificant and is essentially just an adjustment to an unbalanced initial state. A similar conclusion is valid for any localized initial state with parameters satisfying (2.18) (Reznik *et al.* 2001).

The wave field $\tilde{h}_2$ can be found, for example, using a Fourier transform in the space coordinates; the velocity field $(\tilde{U}_2, \tilde{V}_2)$ is obtained from equations (B 21*a*, *b*). One can readily show that

$$\tilde{h}_2, \tilde{U}_2, \tilde{V}_2 = O(1/t), \quad t \to \infty, \quad r, \theta \text{ fixed}, \tag{5.30}$$

i.e. these fields rapidly decay at fixed point with increasing time t.

6. Some properties of the ageostrophic β-gyres

One can show that due to the fast temporal decay of the inertia–gravity wave field (see (5.30)) the fast component $(\tilde{\tilde{X}}_1, \tilde{\tilde{Y}}_1)$ rapidly decays with increasing time t,

$$(\tilde{\tilde{X}}_1, \tilde{\tilde{Y}}_1) = O(1/t), \quad t \to \infty. \tag{6.1}$$

Thus only the slow translation speed correction $(\bar{\dot{X}}_1, \bar{\dot{Y}}_1)$ is dynamically important for times greatly exceeding the inertial time f_0^{-1}. The analysis of the various terms in (5.20) shows that the first three terms on the right-hand side of (5.20) result only in small-amplitude slowly decaying oscillations; the main contribution to a progressive vortex motion is produced by the last sum, here caused by the dipole part of the term $\partial \bar{h}_{21}/\partial\theta$ in (4.12*a*). The terms E_1, E_2 of this sum evolve with a typical orbital time starting from zero at $t = 0$. The term E_3 is time-independent and arises as a result of a rapid relaxation of the field h_2 (equal to zero at the initial moment by virtue of (2.24)) to the stationary dipole $h_{21}^{(3)}$ in (5.18) due to the radiation of inertia–gravity waves. So in the shallow-water model the vortex accelerates practically instantaneously (compared to the typical orbital time) to some finite translation speed.

Analogously to the zero-order translation speed $(\dot{X}_0, \dot{Y}_0)$ the correction $(\dot{X}_1, \dot{Y}_1)$ depends mainly on the dipole part h_2^d of the surface elevation h_2. The dipole term h_2^d, being absent in the QG model (see RGB), will be referred to as the *ageostrophic* β-gyre and is given by the formula

$$h_2^d = \bar{h}_{21}^d + \bar{h}_{22}^d + \tilde{h}_2 \tag{6.2}$$

https://doi.org/10.1017/S0022112001005468 Published online by Cambridge University Press

where $\bar{h}_{22}^d$ is the dipole part of the field $\bar{h}_{22}$ induced by the patch boundary perturbations (see (5.22)),

$$\bar{h}_{22}^d = -\gamma \Phi_1 \operatorname{Im}(\bar{R}_2^{(1)} e^{i\theta}). \tag{6.3}$$

As we have shown the slow part of h_2^d, namely

$$\bar{h}_2^d = \bar{h}_{21}^d + \bar{h}_{22}^d, \tag{6.4}$$

induces a significant translation speed. The rapidly changing dipole $\tilde{h}_2$, consisting of radiating inertia–gravity waves, turns out to be dynamically insignificant because of the fast decay (6.1).

The development of the field $\bar{h}_2^d$ is shown in figure 2(a, b). An interesting feature of this field is its compactness. Unlike the primary β-gyres, where h_1 expands and slowly increases in magnitude with increasing time, the field $\bar{h}_2^d$ is concentrated mainly in the vicinity of the vortex patch, especially for large times; its amplitude tends to some finite value for $T_1 \to \infty$. This difference between h_1 and $\bar{h}_2^d$ is related to a strong localization of the terms in the sum (6.4). The spatial decay of the term $\bar{h}_{22}^d$ is determined by the function $\Phi_1(r)$, which is strongly localized in space (see (4.9b)). The right-hand side of equation (5.15) for $\bar{h}_{21}^d$ is also strongly localized in space and the degree of localization does not depend on time. At the same time the right-hand side, q_0, of equation (5.4a) for h_1, being exponentially decaying in space, 'expands' proportionally to $\ln T_1$ for large T_1 as can be readily seen from (5.2), (5.3).

The polarities of the dipoles $\bar{h}_2^d$ are opposite in sign for the cyclone and anticyclone (see figure 2a, b). One can readily see from this figure that for the case of the cyclone (anticyclone) the dipole $\bar{h}_2^d$ contributes to a positive (negative) zonal translation speed corrections $\dot{X}_1$. Thus the ageostrophic β-gyres force the anticyclone (cyclone) to move faster (slower) in the zonal direction than the analogous vortex in the QG model. This cyclone/anticyclone asymmetry is clearly seen in figure 3 showing the time dependence of $\bar{\dot{X}}_1, \bar{\dot{Y}}_1$. Note that the meridional translation speed correction $\bar{\dot{Y}}_1$ is practically negligible.

The slow sum $h_{21}^{(1)} + h_{21}^{(2)}$ in (5.18) tends to a stationary limit with increasing time T_1, and we can show that

$$E_1|_b \to 2\int_0^1 r h_0 \, \mathrm{d}r - h_0(1), \quad E_1|_b \to 0, \quad T_1 \gg 1. \tag{6.5}$$

At the same time we have from (5.19c) that

$$E_3|_b = h_0(1) - \int_0^1 r h_0 \, \mathrm{d}r. \tag{6.6}$$

Other terms on the right-hand side of (5.20) tend to zero as $T_1 \to \infty$. Therefore, for large times (much exceeding typical orbital times) the translation speed correction is given by the simple equation

$$\bar{\dot{X}}_1 + \mathrm{i}\bar{\dot{Y}}_1 \approx -\int_0^1 r h_0 \, \mathrm{d}r, \quad T_1 \to \infty. \tag{6.7}$$

The limiting speed (6.7) is purely zonal and its sign is negative (positive) for the anticyclone (cyclone).

https://doi.org/10.1017/S0022112001005468 Published online by Cambridge University Press

It is interesting to compare the total translation speed (to this order) $(\dot{X}_0, \dot{Y}_0) + \varepsilon(\dot{X}_1, \dot{Y}_1)$ with the speed of the whole vortex centroid (which is not the same as the vortex *patch* centroid) given by

$$(\dot{X}_{cv}, \dot{Y}_{cv}) = \frac{1}{M_v}\frac{\partial}{\partial t}\int (x, y)\hat{h}\,\mathrm{d}x\,\mathrm{d}y = \frac{1}{M_v}\int h(u, v)\,\mathrm{d}x\,\mathrm{d}y, \tag{6.8a}$$

$$M_v = \int \hat{h}\,\mathrm{d}x\,\mathrm{d}y = \text{constant}, \quad h = h_\infty + \hat{h}. \tag{6.8b}$$

Equation (6.8*a*) is derived using the continuity equation (2.1*c*) written in fixed coordinates. Rewriting (2.1*a*, *b*) (in the same coordinates) in terms of the depth-integrated momentum (hu, hv) one can obtain the following relations (Killworth 1983; Cushman-Roisin, Chassignet & Tang 1990):

$$\frac{\partial}{\partial t}\int hu\,\mathrm{d}x\,\mathrm{d}y - f_0\int hv\,\mathrm{d}x\,\mathrm{d}y = \beta\int yhv\,\mathrm{d}x\,\mathrm{d}y, \tag{6.9a}$$

$$\frac{\partial}{\partial t}\int hv\,\mathrm{d}x\,\mathrm{d}y + f_0\int hu\,\mathrm{d}x\,\mathrm{d}y = -\beta\int yhu\,\mathrm{d}x\,\mathrm{d}y. \tag{6.9b}$$

In our case the contribution of the first-order dipole correction to the integrals on the right-hand side of (6.9) is small and we have

$$\int yhu\,\mathrm{d}x\,\mathrm{d}y \approx -\pi\int_0^\infty r^2 hV_1\,\mathrm{d}r, \quad \int yhv\,\mathrm{d}x\,\mathrm{d}y \approx 0, \quad M_v = 2\pi\int_0^\infty r\hat{h}_I\,\mathrm{d}r. \tag{6.10a, b, c}$$

Using (6.10) one can easily find the components of the total momentum from (6.9) and then the centroid speed from (6.8*a*). Neglecting inertial oscillations one obtains

$$\dot{X}_{cv} \approx \frac{\beta}{f_0}\int_0^\infty r^2 hV_I\,\mathrm{d}r \Big/ 2\int_0^\infty r\hat{h}_I\,\mathrm{d}r, \quad \dot{Y}_{cv} \approx 0. \tag{6.11a, b}$$

Equations (6.11) have previously been obtained in many papers (e.g. Nof 1981; Killworth 1983; Cushman-Roisin, Chassignet & Tang 1990; Benilov 1996). In the quasi-geostrophic approximation we have

$$f_0 V_I \approx g'\frac{\partial\hat{h}_I}{\partial r}, \quad \dot{X}_{cv} \approx -\beta R_d^2, \tag{6.12a, b}$$

i.e. the quasi-geostrophic vortex centroid moves with the drift speed $-\beta R_d^2$ independent of the vortex polarity.

If the depth deviation $\hat{h}$ is small compared to h_∞ but finite as in our case then

$$V_I = \frac{g'}{f_0}\frac{\partial\hat{h}_I}{\partial r} - \frac{1}{f_0}\frac{V_I^2}{r} \approx \frac{g'}{f_0}\frac{\partial\hat{h}_I}{\partial r} - \frac{g'^2}{f_0^3}\frac{1}{r}\left(\frac{\partial\hat{h}_I}{\partial r}\right)^2. \tag{6.13}$$

It readily follows from (6.11), (6.13) that

$$\dot{X}_{cv} \approx \beta R_d^2\left[-1 - \left\{\frac{g'}{f_0^2}\int_0^\infty r\left(\frac{\partial\hat{h}_I}{\partial r}\right)^2\mathrm{d}r + \frac{1}{h_\infty}\int_0^\infty r\hat{h}_I^2\,\mathrm{d}r\right\}\Big/ 2\int_0^\infty r\hat{h}_I\,\mathrm{d}r\right]. \tag{6.14}$$

https://doi.org/10.1017/S0022112001005468 Published online by Cambridge University Press

In non-dimensional form (6.14) is written as

$$\dot{X}_{cv} \approx -1 - \left(\int_0^\infty r \left(\frac{\partial \hat{h}_I}{\partial r} \right)^2 \mathrm{d}r + \int_0^\infty r \hat{h}_I^2 \, \mathrm{d}r \right) \Big/ 2 \int_0^\infty r \hat{h}_I \, \mathrm{d}r. \tag{6.15}$$

It is seen from (6.12*b*) and (6.14) that the second term in the square brackets in (6.14) arises due to ageostrophic effects. This additional term is positive (negative) for the cyclone (anticyclone), i.e. the cyclone (anticyclone) centroid moves westward slower (faster) than the drift velocity. Obviously, equations (6.10) to (6.15) are valid for an arbitrary axisymmetric initial vortex characterized by a small Rossby number.

An important feature of the quasi-geostrophic model is a tendency of the non-stationary lowest-order translation speed to the limiting vortex centroid speed, equal in that case to the drift velocity (6.12*b*) (Reznik 1992; Sutyrin & Flierl 1994; RGB). The analogous property holds in the case under consideration. The lowest-order translation speed (5.7) coincides with the analogous value in RGB and

$$\dot{X}_0 + \mathrm{i}\dot{Y}_0 \to -1, \quad T_1 \gg 1 \tag{6.16}$$

(see equations (5.12), (5.13) of RGB). The second 'ageostrophic' term in (6.15) is exactly equal to the limiting speed (6.7). Therefore the total translation speed $(\dot{X}_0, \dot{Y}_0) + \varepsilon(\dot{X}_1, \dot{Y}_1)$ really tends to the limiting speed $(\dot{X}_{cv}, 0)$ as $T_1 \to \infty$, where $\dot{X}_{cv}$ is given by (6.15). Thus for large time in our model the cyclone (anticyclone) tends to move westward with a translation speed lying inside (outside) the range of the phase velocities of linear Rossby waves. Obviously this property contributes to a greater longevity of anticyclones compared to cyclones, since the Rossby waves radiated by the vortex have a smaller intensity for the anticyclone than for the cyclone.

7. Patch area changes

Two effects of importance arise in the third-order approximation. First, there is the vortex deceleration induced by the secondary geostrophic β-gyres arising as a result of (i) nonlinear interactions between the primary β-gyres and axisymmetric and quadrupole corrections, and (ii) the planetary vorticity advection by the axisymmetric and quadrupole velocity correction fields. This effect was analysed m detail in the quasi-geostrophic model developed in RGB (§7 of RGB). The second new effect arising in the shallow-water model is that the vortex patch area changes in time; in the quasi-geostrophic model it is conserved (see RGB for more detail). This means that in the Fourier series for the successive patch boundary corrections r_m (see the expansion (2.22*e*)),

$$r_m = \sum_{n=0}^{\infty} \mathrm{Im}(R_m^{(n)} \mathrm{e}^{\mathrm{i}n\theta}), \tag{7.1}$$

the coefficient $R_m^{(0)}(t, T_1, \ldots)$ is different from zero for $m = 3, 4 \ldots$, but is zero for $m = 1, 2$. To calculate these terms we use the following third-order equations:

$$\frac{\partial U_3}{\partial t} - V_3 = -\frac{\partial h_3}{\partial r} + F(U)_3, \quad \frac{\partial V_3}{\partial t} + U_3 = -\frac{1}{r}\frac{\partial h_3}{\partial \theta} + F(V)_3, \tag{7.2a,b}$$

$$\zeta_3 - h_3 = \gamma h_2 H(1 - r) + h_{I0} q_1 + (h_{I1} + h_1) q_0 + q_2, \tag{7.2c}$$

https://doi.org/10.1017/S0022112001005468 Published online by Cambridge University Press

$$\zeta_3 = \frac{1}{r}\left[\frac{\partial}{\partial r}(rV_3) - \frac{\partial U_3}{\partial \theta}\right], \tag{7.2d}$$

$$\frac{\partial r_4}{\partial t} + \frac{\partial r_3}{\partial T_1} + \frac{\partial r_2}{\partial T_2} + V_{I0}(1)\frac{\partial r_3}{\partial \theta} + [V_{I1}(1) + V_1|_b + \dot{X}_0 \sin\theta - \dot{Y}_0 \cos\theta]\frac{\partial r_2}{\partial \theta} - \left.\frac{\partial U_1}{\partial r}\right|_b r_2 - U_3|_b + \dot{X}_2 \cos\theta + \dot{Y}_2 \sin\theta = 0. \tag{7.2e}$$

The formulae for $F(U)_3$, $F(V)_3$ are rather cumbersome and so are given in Appendix C.

When azimuthally averaged, equation (7.2*e*) takes the form

$$\frac{\partial r_{40}}{\partial t} + \frac{\partial r_{30}}{\partial T_1} - \langle U_3|_b\rangle + \left\langle V_1|_b \frac{\partial r_2}{\partial \theta} - \left.\frac{\partial U_1}{\partial r}\right|_b r_2 + (\dot{X}_0 \sin\theta - \dot{Y}_0 \cos\theta)\frac{\partial r_2}{\partial \theta}\right\rangle = 0, \tag{7.3}$$

where $r_{k0} = \mathrm{Im}(R_k^{(0)})$, $k = 3, 4$, and the angle brackets denote azimuthal averaging,

$$\langle a\rangle = \frac{1}{2\pi}\int_0^{2\pi} a \,\mathrm{d}\theta.$$

Expressing V_1, U_1, $\dot{X}_0 \sin\theta - \dot{Y}_0 \cos\theta$ in terms of h_1 (see § 5) one can show that the last term in (7.3) vanishes. To find the term $\langle U_3|_b\rangle$ we average (7.2*a–d*) with respect to the azimuth θ and analyse the equations obtained (see Appendix C for details). As a result we have

$$\langle U_3|_b\rangle = -\left.\frac{\partial^2 B_{20}}{\partial r \partial T_1}\right|_b - \tfrac{1}{2}A_{1c}|_b, \tag{7.4}$$

where B_{20}, A_{1c} are given by equations (B 14*b*), (5.5), respectively. By virtue of (B 25) and (7.4) the second and third terms in (7.3) do not depend on the fast time, and therefore we obtain a rather simple formula for the vortex patch expansion rate:

$$\frac{\partial r_{30}}{\partial T_1} = \langle U_3|_b\rangle = -\left.\frac{\partial^2 B_{20}}{\partial r \partial T_1}\right|_b - \tfrac{1}{2}A_{1c}|_b, \tag{7.5a}$$

$$\left.\frac{\partial^2 B_{20}}{\partial r \partial T_1}\right|_b = -\frac{1}{2}\mathrm{Im}\left[I_1(1)\int_1^\infty K_1(r)\bar{A}^*\bar{Q}_0 \,\mathrm{d}r + K_1(1)\int_0^1 I_1(r)\bar{A}^*\bar{Q}_0 \,\mathrm{d}r\right], \tag{7.5b}$$

where $\bar{A}$ and $\bar{Q}_0$ are given by (B 8*d*).

The time dependence of the expansion rate (7.5*a*) is shown in figure 4. One can see that an anticyclonic patch expands and a cyclonic patch contracts, which correlates with a decrease in the absolute value of the depth elevation, as schematically shown in figure 4. It is interesting that the expansion rate (7.5*a*) oscillates strongly in time.

8. Summary and conclusion

We have considered the non-stationary dynamics of an intense localized vortex on the β-plane in a shallow-water model; the vortex is assumed to be axisymmetric at the initial moment. Two interrelated effects are of primary interest: (i) the presence of fast inertia–gravity waves along with the slow Rossby waves, and (ii) the finite deviations of the free surface from its equilibrium position.

Without the β-effect both these effects are insignificant: an arbitrary axisymmetric vortex does not radiate any waves and remains unchanged in time. The β-effect breaks this axial symmetry; therefore with $\beta \neq 0$ the vortex radiates both inertia–gravity and

https://doi.org/10.1017/S0022112001005468 Published online by Cambridge University Press

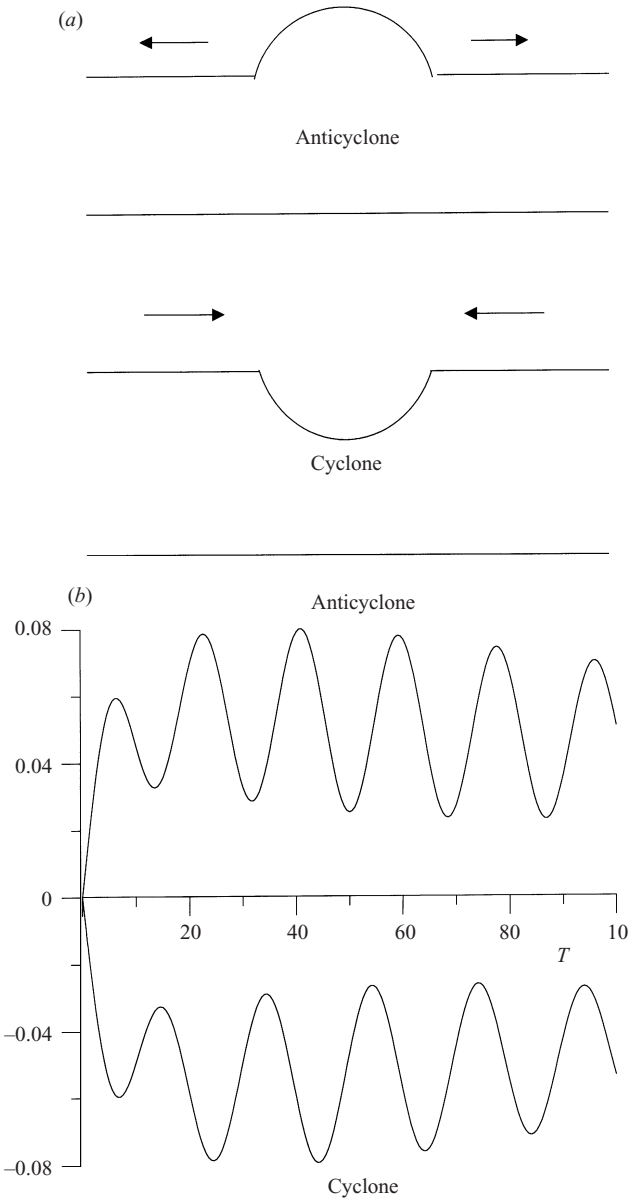


FIGURE 4. The evolution of the vortex patch: (*a*) schematic of evolution due to the decrease of the absolute value of the elevation: for the cyclone the patch contracts, and for the anticyclone it expands; (*b*) the expansion rates of the vortex patch.

Rossby waves and moves along some curved trajectory. To investigate this evolution an asymptotic theory for a vortex with a piecewise-continuous potential vorticity is developed, assuming the Rossby number to be small and the free surface elevation to be small but finite.

Analogously to the quasi-geostrophic model the vortex translation is produced by the secondary dipole circulation (β-gyres) developed in the vortex vicinity. The β-gyres consist of two parts. The first part (geostrophic β-gyres) coincides with the β-gyres in the geostrophic model considered in RGB, and evolves with a typical

https://doi.org/10.1017/S0022112001005468 Published online by Cambridge University Press

swirling time from zero at $t = 0$. A gradual increase of the β-gyre magnitude and size is accompanied by the rise of practically rectilinear uniform flow in the main vortex vicinity, intensifying and expanding with increasing time. Namely this flow advects the vortex along the dipole axis.

The second part (ageostrophic β-gyres) is initiated by the ageostrophic terms in the basic equations. Compared to the geostrophic β-gyres the ageostrophic ones are strongly localized, being confined mainly to the initial vortex vicinity; their amplitude and energy do not grow after some adaptation period. The time evolution of the ageostrophic β-gyres consists of fast and slow stages. During the fast stage the radiation of inertia–gravity waves results in the rapid development of the β-gyres from zero to a dipole field slowly evolving from some non-zero state. Correspondingly, the vortex accelerates practically instantaneously (compared to the typical swirling time) to some finite value of the translation speed. At the next slow stage the radiation is insignificant and the β-gyres change with the typical swirling time.

The total westward translation speed induced by the geostrophic and ageostrophic β-gyres tends with increasing time to the speed of a steadily translating monopole, derived previously in a number of papers. For anticyclones the absolute value of this limiting speed exceeds the absolute value of drift velocity, βR_d^2, of Rossby waves; for cyclones (if one assumes the steadily translating cyclones to exist) it is less. Obviously, this cyclone/anticyclone asymmetry implies that the Rossby waves radiated by the vortex have a smaller intensity for the anticyclone than for the cyclone. In connection with this effect we recall that intense anticyclones steadily translating westward faster than linear Rossby waves can exist in a shallow-water model (see the Introduction). The existence of analogous solutions for cyclones is correspondingly doubtful, since the cyclone propagating with a speed lying in the range of phase speeds of the linear Rossby waves should radiate waves, and hence loses its energy. Our theory generalizes the conclusion about the greater longevity of anticyclones compared to cyclones to the case of non-stationary evolving monopoles.

The influence of inertia–gravity waves upon the vortex evolution was analysed. One can say that the main role of these wave is to provide a 'fast' adjustment to a 'slow' vortex evolution. For large times the inertia–gravity wave field decays rapidly with increasing time at any fixed point. The energy of inertia–gravity waves is negligible compared to the energy of the evolving geostrophic β-gyres.

Yet another peculiarity of the ageostrophic vortex evolution is that the potential vorticity patch changes its area in the course of time. Contraction of a cyclonic patch and expansion of an anticyclonic patch accompany the decreasing in absolute value of the depth elevation.

This work was supported by an ARC Small Grant, and RFBR Grant 99-05-64841. G. M. R. gratefully acknowledges the hospitality of Monash University and University of Warwick where the main part of the work was done. We would like to especially thank Dr Eugene Benilov for his help and advice. We are also grateful to Januscz Zuchowski for his help in computational work.

REFERENCES

Benilov, E. S. 1996 Beta-induced translation of strong isolated eddies. *J. Phys. Oceanogr.* **26**, 2223–2229.

Chassignet, E. P. & Cushman-Roisin, B. 1991 On the influence of a lower layer on the propagation of nonlinear oceanic eddies. *J. Phys. Oceanogr.* **21**, 939–957.

https://doi.org/10.1017/S0022112001005468 Published online by Cambridge University Press

Cushman-Roisin, B., Chassignet, E. P. & Tang, B. 1990 Westward motion of mesoscale eddies. *J. Phys. Oceanogr.* **20**, 758–768.

Davey, M. K. & Killworth, P. D. 1984 Isolated waves and eddies in a shallow water model. *J. Phys. Oceanogr.* **14**, 1047–1064.

Kamenkovich, V. M., Koshlyakov, M. N. & Monin, A. S. 1986 *Synoptic Eddies in the Ocean.* Reidel.

Killworth, P. D. 1983 On the motion of isolated lenses on a beta-plane. *J. Phys. Oceanogr.* **13**, 368–376.

Killworth, P. D. 1986 On the propagation of isolated multilayer and continuously stratified eddies. *J. Phys. Oceanogr.* **16**, 709–716.

Llewellyn Smith, S. G. 1997 The motion of a non-isolated vortex on the beta-plane. *J. Fluid Mech.* **346**, 149–179.

Matsuura, T. & Yamagata, T. 1982 On the evolution of nonlinear planetary eddies larger than the radius of deformation. *J. Phys. Oceanogr.* **12**, 440–456.

McWillams, J. C. 1985 Submesoscale, coherent vortices in the ocean. *Rev. Geophys.* **23**, 165–182.

Nezlin, M. V. & Sutyrin, G. G. 1994 Problems of simulation of large, long-lived vortices in the atmospheres of the giant planets (Jupiter, Saturn, Neptune). *Surveys in Geophys.* **15**, 63–99.

Nof, D. 1981 On the β-induced movement of isolated baroclinic eddies. *J. Phys. Oceanogr.* **11**, 1662–1672.

Nycander, J. & Sutyrin, G. G. 1992 Steadily translating anticyclones on the beta-plane. *Dyn. Atmos. Oceans* **16**, 473–498.

Pedlosky, J. 1979 *Geophysical Fluid Dynamics.* Springer.

Reznik, G. M. 1992 Dynamics of singular vortices on a beta-plane. *J. Fluid Mech.* **240**, 405–432.

Reznik, G. M. & Dewar, W. K. 1994 An analytical theory of distributed axisymmetric barotropic vortices on the β-plane. *J. Fluid Mech.* **269**, 301–321.

Reznik, G. M., Grimshaw, R. & Benilov, E. S. 2000 On the long-term evolution of an intense localised vortex on the β-plane. *J. Fluid Mech.* **422**, 249–280.

Reznik, G. M., Zeitlin, V. & Ben Jelloul, M. 2001 Nonlinear theory of geostrophic adjustment. Part 1. Rotating shallow water model. *J. Fluid Mech.* **445**, 93–120.

Stegner, A. & Zeitlin, V. 1996 Asymptotic expansions and monopolar solitary Rossby vortices in barotropic and two-layer models. *Geophys. Astrophys. Fluid Dyn.* **83**, 159–194.

Sutyrin, G. G. 1994 Long-lived planetary vortices and their evolution: Conservative intermediate geostrophic model. *Chaos* **4**, 203–212.

Sutyrin, G. G. & Dewar, W. K. 1992 Almost symmetric solitary eddies in a two-layer ocean. *J. Fluid Mech.* **238**, 633–656.

Sutyrin, G. G. & Flierl, G. R. 1994 Intense vortex motion on the beta-plane: development of the beta-gyres. *J. Atmos. Sci.* **51**, 773–790.

Williams, G. P. & Yamagata, T. 1984 Geostrophic regimes, intermediate solitary vortices and Jovian vortices. *J. Atmos. Sci.* **41**, 453–478.

https://doi.org/10.1017/S0022112001005468 Published online by Cambridge University Press